RESEARCH ARTICLE

Key Points:
- Data from 14 long-term SHADOZ stations have been reprocessed according to best practices to correct for ozonesonde instrument variability
- Comparisons of total column ozone among reprocessed sonde data and satellite and ground-based instruments agree within 2% for 12 of 14 stations
- In the tropics the 10-station data bias among stratospheric ozone profiles has been markedly reduced and a tropospheric wave-one remains

Correspondence to:
A. M. Thompson,
anne.m.thompson@nasa.gov

First Reprocessing of Southern Hemisphere Additional Ozonesondes (SHADOZ) Ozone Profiles (1998–2016): 2. Comparisons With Satellites and Ground-Based Instruments

Anne M. Thompson[1] iD, Jacquelyn C. Witte[1,2] iD, Chance Sterling[3,4], Allen Jordan[3,4], Bryan J. Johnson[3] iD, Samuel J. Oltmans[3,4], Masatomo Fujiwara[5] iD, Holger Vömel[6] iD, Marc Allaart[7], Ankie Piters[7] iD, Gert J. R. Coetzee[8], Françoise Posny[9] iD, Ernesto Corrales[10], Jorge Andres Diaz[10] iD, Christian Félix[11] iD, Ninong Komala[12], Nga Lai[13], H. T. Ahn Nguyen[13], Matakite Maata[14], Francis Mani[14], Zamuna Zainal[15] iD, Shin-ya Ogino[16], Francisco Paredes[17], Tercio Luiz Bezerra Penha[18], Francisco Raimundo da Silva[18] iD, Sukarni Sallons-Mitro[19], Henry B. Selkirk[1,20] iD, F. J. Schmidlin[21] iD, Rene Stübi[11], and Kennedy Thiongo[22]

[1]Earth Sciences Division, NASA Goddard Space Flight Center, Greenbelt, MD, USA, [2]SSAI, Lanham, MD, USA, [3]Global Monitoring Division, NOAA ESRL, Boulder, CO, USA, [4]Also at CIRES (University of Colorado Cooperative Institute), Boulder, CO, USA, [5]Faculty of Environmental Earth Science, Hokkaido University, Sapporo, Japan, [6]Earth Observations Laboratory, NCAR, Boulder, CO, USA, [7]KNMI (Royal Dutch Meteorological Institute), De Bilt, Netherlands, [8]South Africa Weather Service, Pretoria, South Africa, [9]Laboratoire de l'Atmosphère et des Cyclones, UMR8105 (Université, Météo-France,CNRS), La Réunion, France, [10]Costa Rican National Hangar for Airborne Research Division, National Center for High Technology(CENAT), and Gas Sensing Laboratory, Universidad de Costa Rica, San Jose, Costa Rica, [11]Federal Office of Meteorology and Climatology, MeteoSwiss, Aerological Station, Payerne, Switzerland, [12]National Institute of Aeronautics and Space (LAPAN), Bandung, Indonesia, [13]Ngo Lai, Aero-Meteorological Observatory, National Hydro-Meteorological Service No.8, Hanoi, Vietnam, [14]Division of Chemistry-School of Biological and Chemical Sciences, University of the South Pacific, Suva, Fiji, [15]Malaysian Meteorological Department, Ministry of Science, Technology and Innovation, Petaling Jaya, Malaysia, [16]Japan Agency for Marine-Earth Science and Technology, Research Institute for Global Change, Tropical Climate Variations Research Program, Monsoon Hydrological Cycle Research Team, Yokosuka, Japan, [17]F. Paredes. Instituto Naciona'l de Meteorologi'a y Hidrologi'a, San Cristóbal, Ecuador, [18]Laboratory of Environmental and Tropical Variables, INPE, Brazilian Institute of Space Research, Natal, Brazil, [19]Meteorological Service of Suriname, Paramaribo, Suriname, [20]Also at Universities Space Research Association, Columbia, MD, USA, [21]NASA/GSFC/Wallops Flight Facility, Wallops Island, VA, USA, [22]Kenya Meteorological Department, Nairobi, Kenya

Abstract The Southern Hemisphere ADditional OZonesonde (SHADOZ) network was assembled to validate a new generation of ozone-monitoring satellites and to better characterize the vertical structure of tropical ozone in the troposphere and stratosphere. Beginning with nine stations in 1998, more than 7,000 ozone and *P-T-U* profiles are available from 14 SHADOZ sites that have operated continuously for at least a decade. We analyze ozone profiles from the recently reprocessed SHADOZ data set that is based on adjustments for inconsistencies caused by varying ozonesonde instruments and operating techniques. First, sonde-derived total ozone column amounts are compared to the overpasses from the Earth Probe/Total Ozone Mapping Spectrometer, Ozone Monitoring Instrument, and Ozone Mapping and Profiler Suite satellites that cover 1998–2016. Second, characteristics of the stratospheric and tropospheric columns are examined along with ozone structure in the tropical tropopause layer (TTL). We find that (1) relative to our earlier evaluations of SHADOZ data, in 2003, 2007, and 2012, sonde-satellite total ozone column offsets at 12 stations are 2% or less, a significant improvement; (2) as in prior studies, the 10 tropical SHADOZ stations, defined as within ±19° latitude, display statistically uniform stratospheric column ozone, 229 ± 3.9 DU (Dobson units), and a tropospheric zonal wave-one pattern with a 14 DU mean amplitude; (3) the TTL ozone column, which is also zonally uniform, masks complex vertical structure, and this argues against using satellites for lower stratospheric ozone trends; and (4) reprocessing has led to more uniform stratospheric column amounts across sites and reduced bias in stratospheric profiles. As a consequence, the uncertainty in total column ozone now averages 5%.

1. Introduction

1.1. Design and Features of the SHADOZ Network

The Southern Hemisphere ADditional OZonesonde network (SHADOZ; refer also to Notation below) was initiated in 1998 as an international partnership with both technological and scientific goals that required

Figure 1. Map of SHADOZ stations for which reprocessed data are analyzed in this paper, within the years 1998–2016. Period of operations and sample numbers are in Table 1. Technical details of the reprocessing appear in Witte17a and Sterling17. Details for SHADOZ sondes used at each site during 1998–2004, the Earth-Probe/TOMS period, appear in Thompson, Witte, McPeters, et al. (2003) and Thompson et al. (2007).

augmenting the number of tropical ozone soundings in the troposphere and stratosphere (Thompson et al., 2012; Thompson, Witte, McPeters, et al., 2003; Thompson, Witte, Oltmans, et al., 2003). The ozonesonde data are collected from electrochemical concentration cell (ECC)-type (Komhyr, 1969) sensors launched with a standard radiosonde. Details of ozonesonde-radiosonde pairings used at SHADOZ stations are given in the archival papers (Thompson et al., 2012, hereafter referred to as T12; Thompson, Witte, McPeters, et al., 2003, hereafter referred to as T03; Thompson, Witte, Oltmans, et al., 2003; Thompson et al., 2007, hereafter referred to as T07) and in the companion paper to this one (Witte et al., 2017, referred to hereafter as Witte17a).

The original spatial coverage of SHADOZ was determined by two requirements: (1) that the network consist of existing stations; and (2) full zonal coverage to resolve an equatorial "wave-one" feature observed in satellite total ozone (Fishman & Larsen, 1987; Kim et al., 1996; Shiotani, 1992; Thompson et al., 2000; T03; Thompson, Witte, Oltmans, et al., 2003; Sauvage et al., 2006). At the initiation of SHADOZ in 1998 there were nine stations meeting these criteria, all in the Southern Hemisphere, hence the name of the network (T03). Stations north of the equator joined SHADOZ as follows: Kuala Lumpur (in 1999; Yonemura et al., 2002); Paramaribo (in 1999; Fortuin et al., 2007; Peters et al., 2004); Costa Rica (in 2005; Selkirk et al., 2010); Cotonou (operated 2004–2007; Thouret et al., 2009); Hanoi, where soundings began in 2004 (Ogino et al., 2013). Hilo, Hawaii, with a record extending back to the 1980s, joined SHADOZ in 2009. The 14 stations that have operated at least a decade during SHADOZ and that are covered in this paper appear in Figure 1. More than 7,000 sets of ozone and pressure-temperature-humidity (PTU) profiles from a total of 17 stations that have been part of SHADOZ are available at the website <https://tropo.gsfc.nasa.gov/shadoz>.

For the first 10–15 years of SHADOZ the data were used principally in three ways. First the profiles were used to create climatologies for satellite algorithms (Labow et al., 2015; McPeters & Labow, 2012; McPeters et al., 2007), to evaluate chemical transport models (Kaminski et al., 2008; Martin et al., 2002; Stevenson et al., 2006) and as a reference for coupled chemistry-climate models (Eyring et al., 2005) in intercomparison exercises that support UNEP/WMO Ozone (World Meteorological Organization (WMO), 2007, 2011, 2014) and the Intergovernmental Panel for Climate Change (IPCC) 2007 Assessment. Statistical approaches have been used to create more geographically coherent climatologies (T12; G. Liu, Liu, et al., 2013; J. Liu, Tarasick, et al., 2010, 2013; Tilmes et al., 2012). Self-organizing maps of sondes, in particular, capture meteorological and chemical impacts on profile structure (Jensen, et al., 2012; Stauffer, et al., 2016).

Second, ozone structure near the tropopause has been studied, in the so-called "tropopause transition layer" or "tropical tropopause layer" (TTL; Folkins et al., 2002; Takashima & Shiotani, 2007), with ozone-water vapor relationships captured in the relatively high-accuracy hygrometer data for H_2O (Fujiwara et al., 2001; Vömel et al., 2002). Signatures of convection, waves, and climate oscillations (El Niño–Southern Oscillation (ENSO) and quasi-biennial oscillation (QBO)) dominate ozone interannual variability in the free troposphere (FT) and lower stratosphere (LS). Selkirk et al. (2010) and Thompson et al. (2010) quantified wave impacts on Costa Rican sondes launched during the Tropical Composition, Clouds and Chemical Coupling (TC[4]) campaign. At Ascension, even though convection is less prevalent than over the western Pacific and Indian
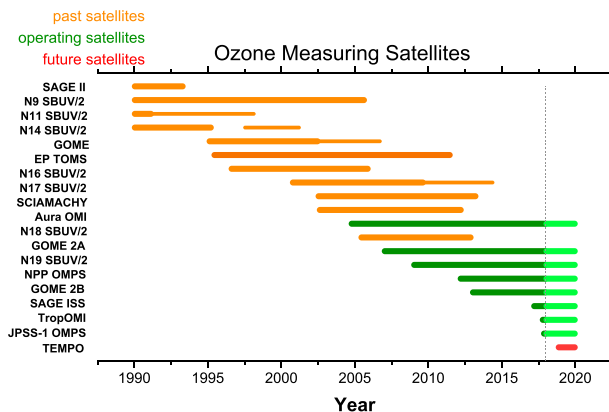
Figure 2. Timeline of satellite ozone instruments that have used SHADOZ for validation. Beyond 2017, expected lifetime for operational sensors is indicated in light green. TEMPO (in red) scheduled for U.S. launch.

Oceans, profiles with the lowest mean tropospheric ozone mixing ratio display an S shape year-round (T12). This is presumably a combination of the regional subsidence along with convection in some months (Figure 4 in Jensen et al., 2012; Figures 4 and 8 in T12). In Thompson, Allen, et al. (2011) gravity waves were identified through ozone laminae within the upper troposphere (UT) and TTL. A gravity wave index constructed for 12 SHADOZ stations captured responses to ENSO episodes.

Third, satellites use SHADOZ profiles for validation of tropospheric and/or stratospheric data (e.g., Aura validation; Special Issue of *Journal of Geophysical Research*, 2007–2008) and newer sensors like Ozone Mapping and Profiler Suite (OMPS) on Suomi-NPP (National Polar-Orbiting Partnership), Infrared Atmospheric Sounder Instrument (IASI), and Global Ozone Monitoring Experiment-2 (GOME-2) (Figure 2). SHADOZ data have also been used to derive ozone trends (Heue et al., 2016). In Randel and Thompson (2011) a composite SAGE II and SHADOZ data set (1984–2009) for ozone over eight equatorial stations defined a lower stratosphere (LS) trend of −2 to −4%/decade. Two subtropical sounding stations with data prior to the start of SHADOZ, Irene and La Réunion, displayed large positive trends in FT ozone, not in summer or spring, when biomass fires are widespread, but in winter (Thompson et al., 2014). In Gebhardt et al. (2014), combined Scanning Imaging Absorption SpectroMeter for Atmospheric ChartographY (SCIAMACHY) and SHADOZ data for 2002 to 2012 show flat to slightly increasing ozone in the equatorial LS. Hubert et al. (2016) employed sonde profiles to evaluate satellite drift over the past 10–15 years. To date, it appears that most operational satellites (14 limb sounders were evaluated by Hubert et al., 2016) are quite stable in the lower and middle stratosphere. To be used as references for satellite drift evaluation, the sonde precision needs to be 3–5%, somewhat better than the level achieved in the past 10–15 years.

1.2. Quality Assurance: Technological Aspects of SHADOZ

An essential technological goal of SHADOZ is to adopt, when appropriate, recommendations for sonde technique and data processing when researchers have used laboratory and field test results to produce consensus-based recommendations for data handling. The beginning of SHADOZ coincided with a series of JOSIE (Jülich [Germany] Ozonesonde Intercomparison Experiments) in test chambers (Smit & Kley, 1998; Smit & Straeter, 2004), as well as laboratory studies elsewhere (Johnson et al., 2002). ECC ozonesonde manufacturers modify materials from time to time (Komhyr, 1986; Komhyr et al., 1995), and several variations of the potassium iodide sensing solution that reacts with ozone molecules are widely used (Witte17a). Furthermore, the motor-driven Teflon piston pump that draws air into the cells of the ECC instrument drops in efficiency as the sonde ascends into the stratosphere. Several groups have employed different formulae to correct for this effect, in a "pump efficiency correction factor" or PCF. Thus, different combinations of instrument manufacturer, sensing solution type (SST), and PCF can lead to divergent values of ozone partial pressure. These variations prompted the World Meteorological Organization (WMO) to support the formation of the World Ozonesonde Calibration Chamber System (Smit & Kley, 1998) in Jülich and, starting in 1996, to sponsor the JOSIE series of chamber tests. In JOSIE experiments to date, different types of sondes, not all of them ECC, measured ozone introduced into the chamber at changing temperatures and pressures that simulate a balloon ascent to 10 hPa. A UV photometer (Proffitt & McLaughlin, 1983) supplies the reference ozone measurement to which the sonde reading is compared.

The JOSIE-2000 campaign (Smit et al., 2007) accommodated SHADOZ by testing combinations of instrument type and SST in chamber simulations that followed the temperature and typical ozone trace of a tropical sounding. Clear biases from differences in the instrument manufacturer (there are basically two ECC hardware types) and SST were apparent. In 2004 the Balloon Experiment on Standards for Ozone Sondes (BESOS) field campaign, conducted in Wyoming, USA, with a standard UV photometer and a gondola of 18 ozonesondes on a large balloon, displayed similar biases among sonde types (Deshler et al., 2008). These intercomparison activities led to recommendations of certain ozonesonde instrument-SST combinations for more consistent sonde results and served as the basis for WMO/GAW (Global Atmospheric Watch)

standard operating procedures (Smit & Panel for the Assessment of Standard Operating Procedures for Ozonesondes (ASOPOS), 2014). Several SHADOZ stations modified their technique and/or reprocessed data during the period 2000–2005, improving agreement between total ozone values from the sondes and colocated ground-based instruments and total ozone satellite instruments (T12; T07) relative to the first comparisons in T03. JOSIE and related activities have reduced the total uncertainty of the sonde measurement from ~15–20% to 5–10% (WMO, 2007, 2011). Nonetheless, SHADOZ total ozone column amounts referenced to satellite (Total Ozone Mapping Spectrometer (TOMS) or Ozone Monitoring Instrument (OMI)) columns as well as stratospheric ozone columns from the sondes indicated station-to-station biases (T12; T07). Some of the biases followed discrepancies associated with variations in SST and instrument that were identified in JOSIE and BESOS.

1.3. Ozonesonde Reprocessing: Goals of This Study

Since 2010, workshops of the SI2N (SPARC-IO3C-IGACO-NDACC) activity and a series of Ozonesonde Experts Meetings have led to recommendations on how to reprocess soundings to compensate for the range of instrument type, SST, and various choices of background current and PCF (Smit & ASOPOS, 2012). An important element of reprocessing data from different SST and ozonesonde instruments is to homogenize data with a "transfer function." Deshler et al. (2017) supply transfer functions for the major combinations of instrument type and SST. At present six to eight providers of ozonesonde data, representing ~30 stations globally, have adopted the guidelines. Papers describing the reprocessing of Canadian network data (Tarasick et al., 2016) and two European records (van Malderen et al., 2016) have appeared. In the past 2 years we have been reprocessing the SHADOZ profiles for 14 stations that have records of at least 10 years within the period 1998–2016. The basis for the reprocessing is Smit and ASOPOS (2012) with some modification for several stations as described in section 2. Details for the reprocessing of data from the first seven stations appear in Witte17a. Additional reprocessing, including for an eighth station, are given, along with ozone profile and column uncertainties in J. C. Witte et al. (First reprocessing of Southern Hemisphere ADditional Ozonesondes (SHADOZ) profile records: 3. Uncertainty in ozone profile and total column, submitted to *Journal of Geophysical Research: Atmospheres*, 2017, https://doi.org/10.1002/2017JD027791, hereafter referred to as Witte17b). The complete reprocessed SHADOZ data set will be released as SHADOZ v6.0. The present study evaluates the reprocessed data to date and addresses the following:

1. How do total column ozone (TCO) amounts for the SHADOZ stations agree with satellite TCO in the period 1998–2016? How do the sonde ozone columns compare to colocated Dobson, Brewer, and System d'Analyze par Observation Zenitale (SAOZ) instruments at nine SHADOZ stations?
2. How do stratospheric, tropospheric, and TTL column ozone amounts for the tropical stations (defined as within ±19° of the equator), calculated from the reprocessed data, compare to one another? Are the stratospheric and TTL ozone columns zonally uniform? What is the variability in TCO after reprocessing?
3. What are tropospheric column ozone amounts at each station with the reprocessed data? What is the magnitude of the wave-one pattern in tropospheric ozone?
4. Using a mean reference profile from the tropical SHADOZ stations, are there station biases in stratospheric ozone? Have biases changed from T07 and T12?

We summarize operating characteristics of all SHADOZ stations (section 2) and present the results in section 3. Section 4 is a summary.

2. Data and Methods of Analysis

2.1. SHADOZ and Other Ozone Instrumentation

The 14 SHADOZ sites (Figure 1) launch two to four times per month mostly between 0800 and 1400 local time. Table 1 presents station location and numbers of soundings that are used in our analyses, along with independent total ozone instrumentation. The station labeled as Costa Rica represents sonde launches near San Jose, the capital, that have changed location several times since late 2005.

SHADOZ archives ozone profiles with records of temperature, pressure, and relative humidity from standard radiosondes. Over the 19 year record covered here, Vaisala RS-80, RS-92, MW-41, and Internet (iMet) radiosondes have been used at most stations (Table 2). Exceptions are Réunion, where a Meteo Modem radiosonde has been employed, and Kuala Lumpur where various ozonesonde-radiosonde combinations

Table 1

SHADOZ Stations With Colocated Ground-Based Total Ozone Instrument (Where Applicable) and Sample Numbers (Total Reprocessed Records With Bursts Between 10 and 15 hPa)

| Station name	Location	Local launch times[a]	Ground total ozone instrument	Profile #	Reprocessing reference
American Samoa	14.23°S, 170.56°W	0800–1200, 1300–1800	Dobson #80	480	Sterling17
Hilo, Hawaii	19.40°N, 155.0°W	0800–1300	---	600	Sterling17
San Cristóbal, Galapagos (Ecuador)	0.92°S, 89.60°W	0500–1700	---	387	Sterling17
Costa Rica (various sites)[b]	9.94°N, 84.04°W	0600–1200	---	440	Witte17, this study
Paramaribo, Surinam	5.81°N, 55.21°W	0900–1400	Brewer #159	476	Allaart et al., in prep., *Atmospheric Measurement Technology (AMT)*
Ascension Island, UK	7.98°S, 14.42°W	1300–1400	---	538	Witte17a
Natal, Brazil	5.42°S, 35.38°E	1200–1400	Dobson #93	517	Witte17a
Irene, South Africa	25.9°S, 28.22°E	1000–1300	Dobson #89	258	Witte17a
Nairobi, Kenya	1.27°S, 36.80°E	0700–1800	Dobson #18	719	Witte17b
La Réunion, France	21.1°S, 55.48°E	0800–1300	SAOZ#20	521	Witte17a,b with modification described in sec 2.2
Kuala Lumpur, Malaysia	2.73°N, 101.7°E	1000–1200	Brewer #90	271	Witte17a
Hanoi, Vietnam	21.02°N, 105.80°E	1300–1400	Brewer #208	148	Witte17a
Watukosek-Java, Indonesia	7.57°S, 112.65°E	1200–1300	Brewer #116 in Bandung	146	Witte17a
Suva, Fiji	18.13°S, 112.65°E	0800–1100, 2100–2300	--	222	Sterling17

Note. Reference for reprocessing is also given.
[a]Average times. [b]Current site is San Pedro. Alajuela and Heredia historic sites are within 0.5° of San Pedro.

appear with four different radiosonde manufacturers. The Lockheed-Martin Sippican radiosonde, a successor to Viz, is used at Natal and was employed at Ascension from 1998 to mid-2010. When Ascension launches resumed in March 2016, EnSci ozonesondes replaced Science Pump Corporation (SPC) instruments and an iMet radiosonde was used. Details of each station's equipment are found at <http://tropo.gsfc.nasa.gov/shadoz>; every record's metadata lists instrument type and usually serial number for ozonesonde and radiosonde. Details of the SHADOZ radiosonde/ozonesonde systems for seven stations appear in Witte17a. In the case of Watukosek, only data from mid-2001, taken using Strato software with EnSci ECC and RS80 sondes, have been reprocessed (reprocessing of 1999–2001 EnSci/RS-80 data with a V03 data system is pending). Hilo, Fiji, Samoa, and San Cristóbal sondes, reprocessed by C. W. Sterling, B. J. Johnson, S. J. Oltmans et al. (Homogenizing and estimating the uncertainty in NOAA's long term vertical ozone profile records measured with the electrochemical concentration cell ozonesonde, submitted to Atmospheric Chemistry and Physics Discussions, 2017:597; reprocessing method referred to as Sterling17 in Table 1), switched from Vaisala RS-80 radiosondes to iMet or RS-92 after 2010. Table 2 shows the time period of each radiosonde at the nine stations where there have been changes. For comparisons with satellite and ground-based total ozone instruments, data compromised by balloon bursts lower than 15 hPa are not used. Above

Table 2

Radiosondes Used at SHADOZ Stations

	RS80 or RS92	Pressure offset correction	iMet	Pressure offset correction
Samoa	RS80: 1998–2013	No	10 January 2014 to present	Yes
Fiji	RS80: 1998–2013	Intermittent	2015 to present	Yes
Hilo	RS80: 1998 to 5 September 2012	Intermittent; yes after 8 April 2009	12 September 2012 to 28 November 2012	No
			5 December 2012 to present	Yes
San Cristóbal	RS80: 1998–2008	No	---	---
	RS92: May 2012 to present	Yes		
Costa Rica[a]	RS80: 2005 to 16 August 2013	Yes; Vömel method[b]	19 August 2010 to present	Yes
Paramaribo	RS80: 1999 to 17 September 2005	No	---	---
	RS92: 3 October 2005 to present			
Nairobi	RS80: 1998 to 3 March 2010	No	---	---
	RS92: 9 June 2010 to present			
Ascension			2016 to present[c]	Yes

[a]Overlap of iMet and RS80 between August 2010 and August 2013. [b]Using rise rate. [c]LMS: 1998–2010 (refer to Witte17a).
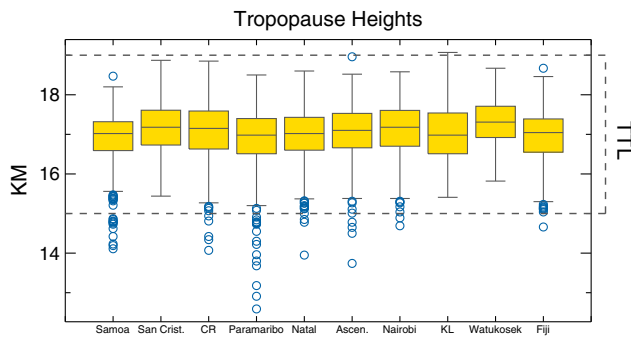
Figure 3. Box-and-whisker plot of tropopause heights is shown for the 10 SHADOZ stations within ±19° of the equator, designated as "tropical." Yellow boxes show the interquartile of the 25th, median, and 75th percentiles. Outliers are displayed as blue circles. The TTL region is bounded by the dashed lines.

10 hPa or burst, extrapolation to total column is made with the climatology of McPeters and Labow (2012). No normalization to the total ozone reading of a satellite or ground-based instrument is made. Ground-based data are taken from the World Ozone and Ultraviolet Data Centre (WOUDC) and Network for Detection of Atmospheric Composition Change (NDACC) public archives.

Sonde total ozone comparisons are made with satellite measurements from three instruments of similar design that operated in the 1998–2016 period (Figure 2). These are NASA's Earth Probe/TOMS (Total Ozone Mapping Spectrometer) instrument, covering sonde launches from January 1998 to September 2004; the Dutch/Finnish OMI (Ozone Monitoring Instrument) on board NASA's Aura spacecraft (September 2004 to the present); and OMPS (Ozone Mapping Profiler Suite) on the NASA-National Oceanic and Atmospheric Administration (NOAA) Suomi-National Polar-orbiting Partnership from February 2012 to the present. In the latter period both OMI and OMPS overpass total ozone are used; there are more OMPS measurements because of post-2008 degradation in the OMI detector array. Not every sonde record is evaluated with the satellite because overpass data are screened for cloudiness greater than 60% and the satellite distance is limited to <200 km.

2.2. Reprocessed Ozonesonde Data

A summary and reference for the reprocessing of each station appears in Table 1. Details for seven stations that were reprocessed at NASA/Goddard appear in Witte17a: Natal, Ascension, Irene, La Réunion, Kuala Lumpur, Hanoi, and Watukosek (Figure 1). In Witte17a, comparisons of sonde total ozone for 1998–2015 with TOMS and OMI satellites are made with original (SHADOZ version 5.2) and reprocessed data to demonstrate improvements in the satellite-sonde offset. Also, in Witte17a midstratospheric ozone from the sonde profiles before and after reprocessing is compared to coincident Aura/MLS (Microwave Limb Sounder) data from September 2004 to 2015. Notable improvements appear between 65 hPa and 10 hPa for six of the seven stations. Since Witte17a was completed, we added all the 2016 reprocessed SHADOZ data to our seven-station reprocessing and completed reprocessing of Nairobi data (Witte17b). Witte17a has since reprocessed Costa Rica data in the same way. A transfer function, developed by Deshler et al. (2017), was applied to the La Réunion data after 2007 to correct for a solution change. These data are now homogenized to an EnSci/0.5%, half buffer SST (Witte17b).

The four stations with data reprocessed by the NOAA ESRL/GMD Ozone group (Hilo, Samoa, San Cristóbal, and Fiji) used a 2.0% unbuffered SST with EnSci's for the 1998–2005 period, after which they switched to a 1.0% 1/10 buffer SST (Sterling17; Table 1). The 1998–2005 data have been reprocessed in the same way as the Watokusek data that are based on the EnSci/2.0% unbuffered SST (Witte17a). A transfer function based on Deshler et al. (2017) is applied to the San Cristóbal 1998–2006/11/02 data to convert ozone measurements made with a SPC/6A sonde to an EnSci/Z equivalent. This gives roughly a 4% increase in the ozone profile measurements.

Paramaribo data have been reprocessed by Royal Dutch Meteorological Institute (M. Allaart and A. Piters, personal communication, 2017) according to the O3S-DQA (Smit & ASOPOS, 2012) guidelines; where background currents required adjustment, the guideline of Newton et al. (2016) was followed.

2.3. Analyses: Tropopause and TTL Definitions

In the analyses that follow, we refer to the TTL and the tropopause, terms that sometimes vary from one study to another. The TTL is defined as a region in which both tropospheric and stratospheric properties are found in terms of constituent mixing ratios and temperature gradients, wave activity, radiative heating rates, and other thermodynamic quantities (Fueglistaler et al., 2009; Gettelman & de F. Forster, 2002). We adopt 15–18.5 km for the TTL (Figure 3) that encompass the minimum and maximum tropopause values for tropical sites within 19° of the equator. This range is ~1 km higher than Fueglistaler et al. (2009). However, our TTL definition encompasses the locations of the tropical cold-point tropopause (CPT, Selkirk et al., 2010), the thermal lapse rate tropopause, and the ozonopause, that is, an ozone tropopause defined

as the height at which there is a sharp gradient in ozone concentration at the base of the stratosphere (Bethan et al., 1996; Sivakumar et al., 2011; T12). We use the Bethan et al. (1996) definition for the tropopause. The values in Figure 3 are virtually identical for 10 stations, averaging 17.1 km, and there are few tropopause heights below 14 km.

3. Results and Discussion

3.1. Sonde Total Ozone Columns Compared to Ground-Based Instrument and Satellite Overpass Total Ozone

For the 14 stations Figure 4 shows a time series of integrated total ozone from the sonde (red) and the daily TOMS/OMI/OMPS overpass total. The order of the individual panels is west to east by longitude, starting at 180 W longitude. The satellite total ozone from TOMS appears in dark gray, OMI total ozone is in black, and OMPS total ozone is in silver. For nine stations (Table 1) total column ozone from a colocated instrument, a Brewer spectrometer, a Dobson, or SAOZ, is also shown in Figure 4 (blue). The bottom panel of each time series summarizes the ratio of sonde total ozone to the corresponding satellite overpass or ground-based measurement. At the right in each figure there is a histogram of offsets between the sonde total from the reprocessed data and the satellite (yellow). There are five stations without ground-based total ozone instruments: Ascension, Hilo, San Cristóbal, Costa Rica, and Fiji. For the nine stations with ground-based instruments, a histogram of the sonde total and the ground-based instrument ozone total (hatched in Figure 4) also appears in the right panel. Comparisons of total ozone from the ground-based instrument and the concurrent satellites appear in Figure 5. In Figure 4 sonde and satellite comparisons display a high fraction of near-zero differences for every station except two data sets where the distribution peaks are skewed closer to +5% (Paramaribo) and −5% (Kuala Lumpur). All but two of the sonde-satellite discrepancies show the sonde total to be lower than the satellite (Table 3), similar to prior SHADOZ satellite-sonde total ozone comparisons (T12; T03; T07; Witte17a).

Among the 14 stations all but Kuala Lumpur and Paramaribo have an average agreement with the satellite overpasses within 2% absolute or better (Table 3, fourth column). This represents a significant improvement over the sonde data currently archived, as described in Witte17a (Table 4) and Sterling17. Overall, sonde-satellite agreement is improved relative to the total ozone comparisons in T07 (EP (Earth Probe)/TOMS satellite reference, for sondes launched in 1998–2004) and in T12 (Figure 11, for OMI comparisons, 2005–2009).

3.1.1. Sonde-Satellite-Ground-Based Time Series at Individual Stations

Samoa is one station for which the total ozone agreement has improved considerably since the T03 evaluation where the sonde-TOMS ozone offset, based on 1998–2000 soundings, was ~10%. For 1998–2004, with some instrument and sensing solution changes after JOSIE-2000 (Smit et al., 2007), satellite and Dobson comparisons implied that the sondes were 5–7% too low (T07). Reprocessing improves the satellite agreement on average, from 1998 to 2016, to 0.9% mean difference (fourth column in Table 3). The Dobson total ozone also agrees well with the sonde TCO. This is seen in the histograms in the right panel of Figure 4a that display a relatively tight and Gaussian distribution of sonde-satellite (yellow) and sonde-Dobson (hatched) total ozone.

Referring to the bottom panel in Figure 4a, the sonde/TOMS ratio (1998 to late 2004) averages 0.97–0.98. There are other features to note with the Samoa data (Figure 4a). First, the sonde/Dobson ratio for 1998 to late 2004 is slightly higher than sonde/TOMS. This implies that TOMS total ozone is greater than the Dobson; that is consistent with the Dobson/TOMS ratio peaking at less than 1.0 in Figure 5a (yellow shading). Second, from 2006 to 2010 in the OMI period, the sonde/Dobson ratio and sonde/OMI are both closer to 1.0 (Figure 4a) than the 1998–2004 sonde-Dobson-TOMS comparisons (T07). This too agrees with the Dobson/OMI total ozone ratio peaking near unity in Figure 5a (blue hatched). Third, the close sonde-satellite-Dobson agreement continues into mid-2014, when most of the sonde-satellite comparisons are based on OMPS. The ratios, both sonde/OMI and sonde/OMPS, declined on average from late 2014 to 2016. During OMPS there are many Dobson comparisons with the satellite (Figure 4a) but few sonde comparisons with the Dobson. The Dobson/OMPS (green hatched in Figure 5a) peaks slightly lower than the Dobson/OMI but it is higher than Dobson/TOMS.

In Figure 4b for Hilo (elevation 10 m), only satellite comparisons are displayed because the nearby Dobson spectrometer at Mauna Loa is 3.4 km above mean sea level. Hilo displays one of the best homogenized
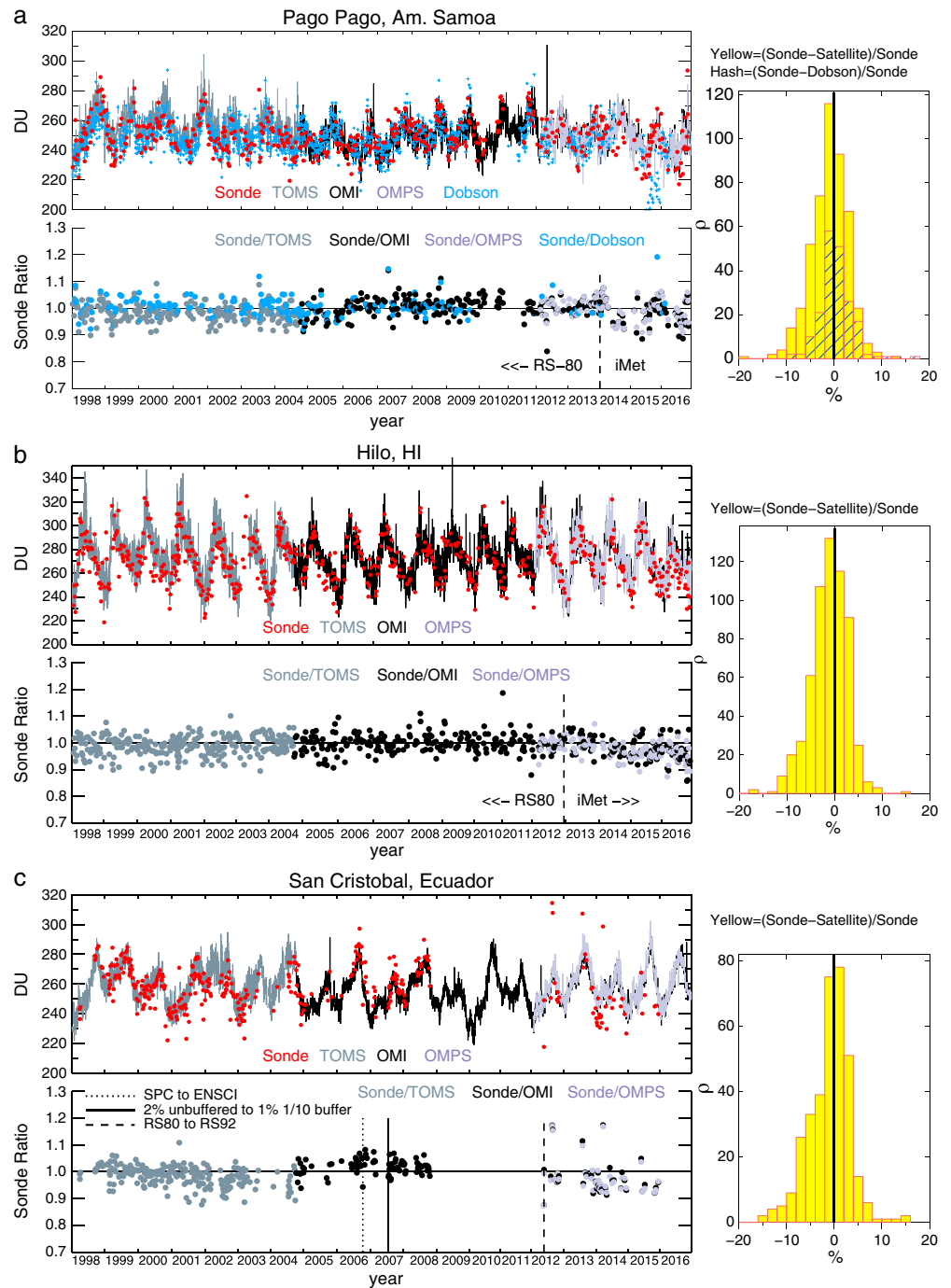
Figure 4. Time series of TOMS-OMI-OMPS overpass total column ozone (O$_3$, gray-black-silver lines, respectively) with ozonesonde total column O$_3$ (red circles) values that reached 10 hPa. McPeters and Labow (2012) O$_3$ climatology is added from 10 hPa to the top of the atmosphere to yield sonde total column amounts. After February 2012 OMI and OMPS operated simultaneously. Where available, total column O$_3$ from colocated Dobson, Brewer, or SAOZ instruments (blue cross) is given. The bottom panel includes sonde/satellite and sonde/ground instrument ratios. Here too, after February 2012, sonde/satellite ratios include both OMI (black circles) and OMPS (silver circles). Histograms of the percent difference with respect to sondes are also given for each station (yellow). Where available, the percent difference is also shown between the sondes and ground-based total column O$_3$ (blue hatched). (a) American Samoa; (b) Hilo, Hawaii; (c) San Cristóbal; (d) Costa Rica; (e) Paramaribo; (f) Natal; (g) Ascension; (h) Irene; (i) Nairobi; (j) Réunion; (k) Kuala Lumpur; (l) Hanoi; (m) Watukosek; (n) Fiji. Satellite overpasses are filtered for reflectivity greater than 0.6 and distance from the station location greater than 200 km.
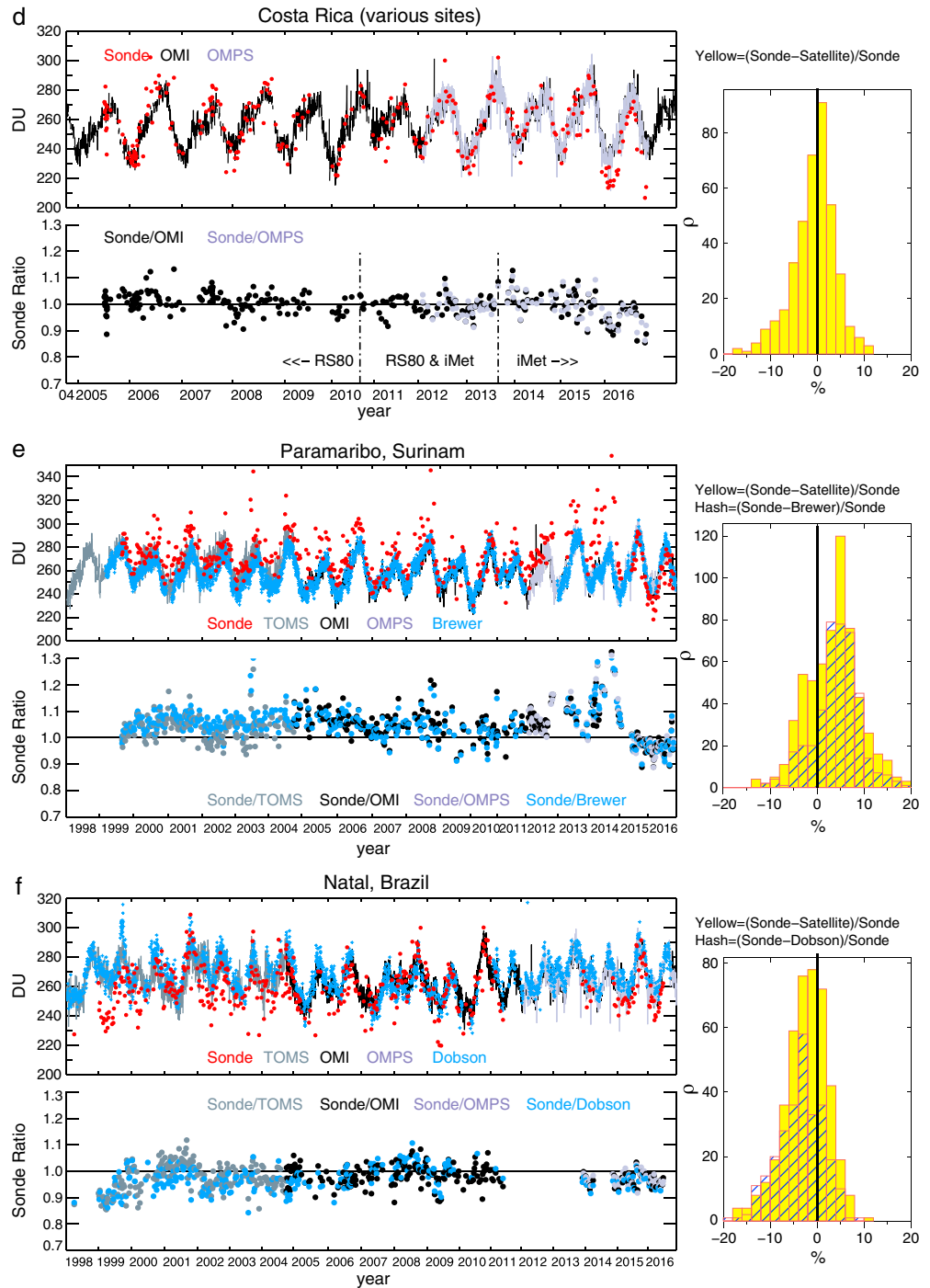
Figure 4. (continued)

sonde records throughout the SHADOZ period. Because of its northern subtropical location, there is a large variation in total ozone, close to 100 Dobson units (DU) in a highly regular cycle (see also Figure 10e in T12). Maximum total ozone over Hilo is from February to May (Oltmans et al., 2004; T12) during which the UT/LS displays extratropical ozone-rich air and a lower tropopause (Figure 3b in T12). In contrast, July–September is characterized by lower ozone throughout the free troposphere with a midtroposphere minimum that resembles boundary layer Hilo ozone (Figure 3b in T12), suggestive of convective mixing. The Hilo-satellite comparisons (Figure 4b) show similar patterns to the Samoa (Figure 4a) sonde ratios. For the
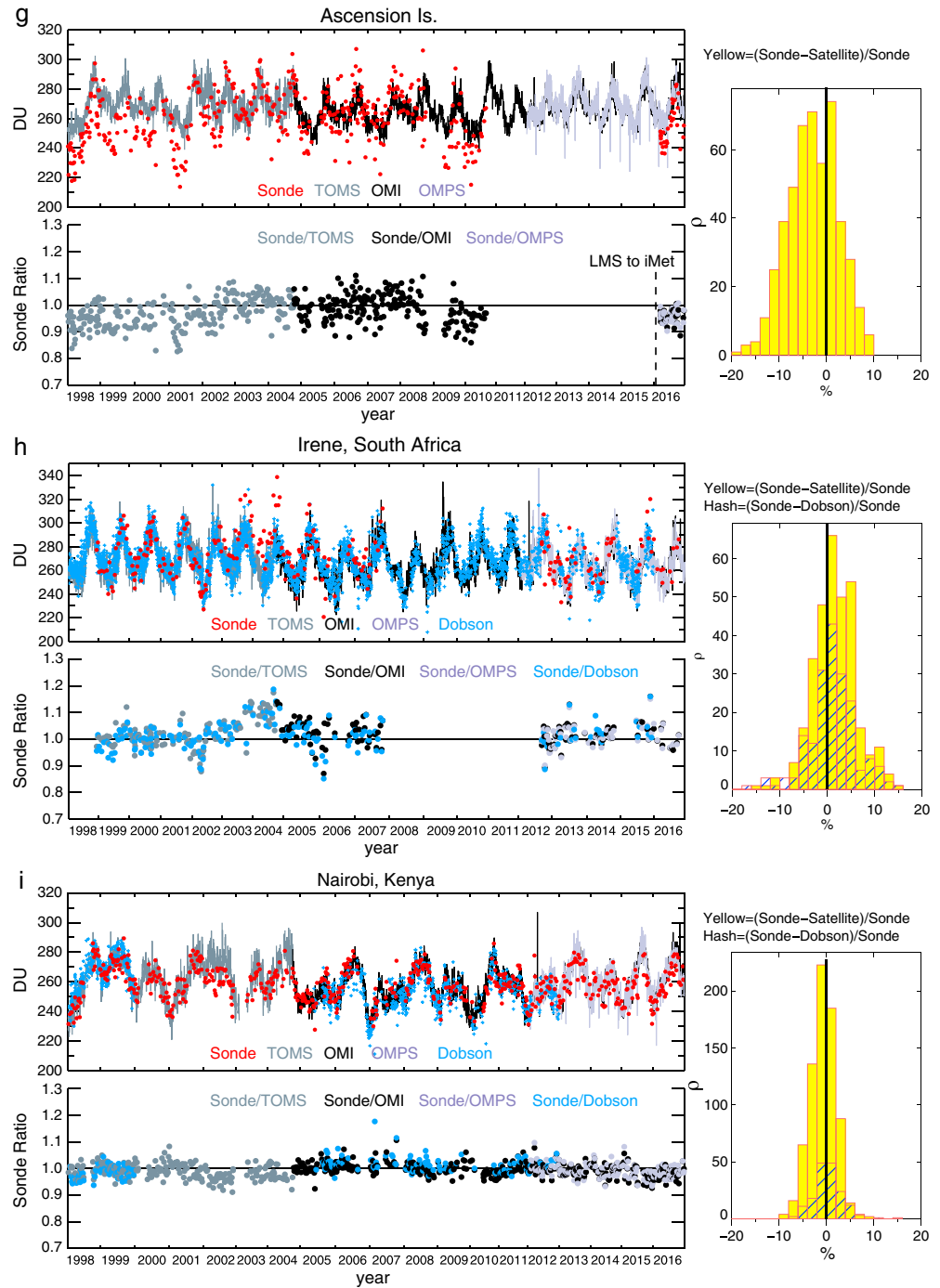
Figure 4. (continued)

TOMS to early OMI period, 1998–2005, the Hilo ratios average an equivalent of 1–2% lower ozone than the satellites (Figure 4b). After that, up through 2013, the sonde/satellite ratio clusters about 1.0, with nearly all data within 0.95–1.05. In the first 2 years of the OMI-OMPS overlap the sonde-satellite ratio resembles the 2004–2011 record. In mid-2014, as with Samoa, Hilo sonde ratios decline several percent with a number of values falling below 0.9. This pattern is reflected in the histogram of satellite to sonde offsets (yellow in Figure 4b, right). The tail of negative values, corresponding to sonde lower than satellite, extends almost to −20%. However, the overall sonde-satellite difference is −1.2% (Table 3, sonde lower).
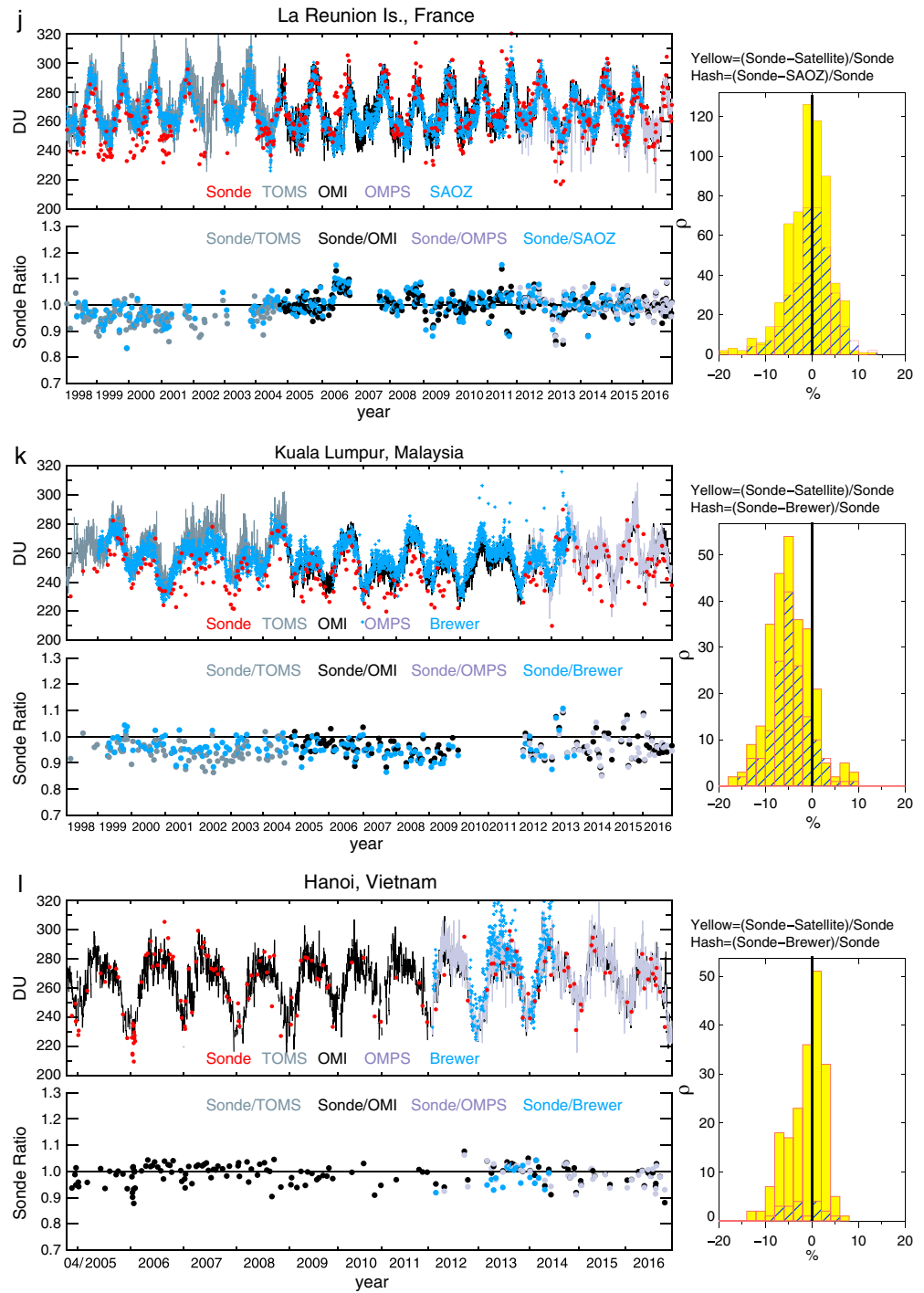
Figure 4. (continued)

In Figure 4c the San Cristóbal time series displays several data gaps, for example, no launches in 2009–2011, with a drop in launch frequency in 2012–2015. The sonde/satellite ratios for the TOMS and early OMI era (1998–2005) averages 0.93. As with Samoa and Hilo (Figures 4a and 4b), the sonde/OMI ratio for 2006–2008 exceeds 1.0, but in 2012–2015, the ratio drops to ~0.95. The San Cristóbal histogram (Figure 4c, right) skews toward −20%, but 80% of the differences are close to 0, averaging a −0.9% offset; that is, sondes have lower ozone.
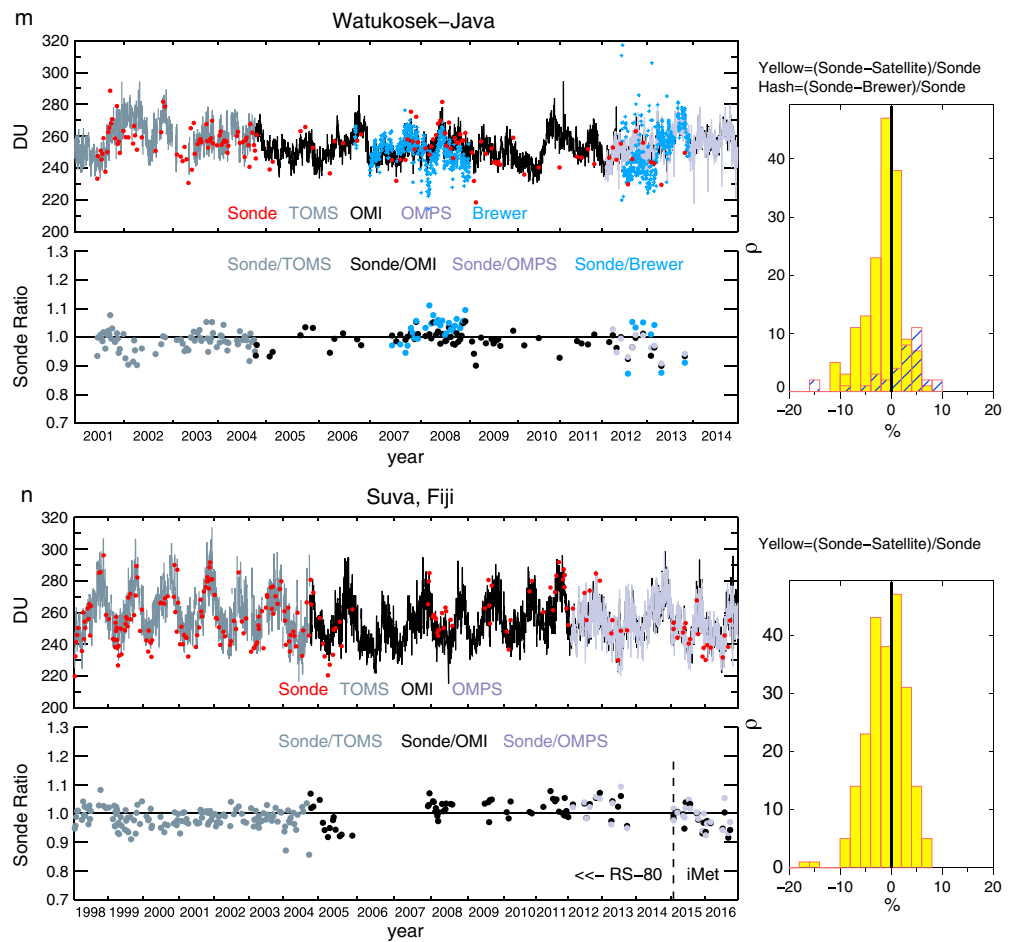
Figure 4. (continued)

The Costa Rican sondes that started in 2005 (Figure 4d) span the OMI and OMPS periods. They suggest a pattern somewhat different from the three Pacific stations illustrated in Figures 4a–4c. In 2005 through most of 2007 the ratio is frequently greater than 1.0. From late 2007 to early 2015 ratios span 0.9 to 1.07, during which there seem to be two distinct phases. From late 2007 to early 2014 the ratios are predominantly less than 1.0, followed by many values >1.0 after mid-2012 (note that more statistics partly result from frequent OMPS overpasses). After 2014, although the percentage of sonde/satellite ratios greater than 1.0 increases, the distribution shifts to more values <0.9. In 2016 there are many sondes with ratios 0.80–0.90. The Costa Rica histogram (Figure 4d, right) displays negative values to −20%, but the overall mean relative to OMI and OMPS is −0.2% (fourth column, Table 3).

The sondes at Paramaribo (Figure 4e) represent the only reprocessed data set for which the sondes display markedly higher ozone than the satellites and the ground-based instrument for most the period 1999–2016. Paramaribo is the SHADOZ station with the second largest ground-based data set; the Brewer/satellite ozone ratios in Figure 5b are based on more than 5,000 coincidences. Comparisons of Brewer total ozone with the three satellites agree well; as for Samoa (Figure 5a), the ozone from the ground-based instrument relative to the satellite varies among the three satellites at Paramaribo. TOMS has highest ozone (lowest ratio, yellow in Figure 5b) with sonde/OMI somewhat higher than sonde/OMPS. In Figure 4e, between 2011 and 2014 there is an almost monotonic increase in the sonde/satellite ratios that disappears by 2015. These persistent positive ratios, interpreted in the past as signifying a bias at Paramaribo relative to profiles of the other nine tropical stations (Figure 13b in T12), disappear after 2015. Then the sonde/ satellite (OMI and OMPS) and sonde/Brewer ratios more closely resemble the four stations discussed above. Around 2015 there was a change in the sonde sensing solution; the data are being reprocessed again (A. Piters and M. Allaart, personal communication, 2017).
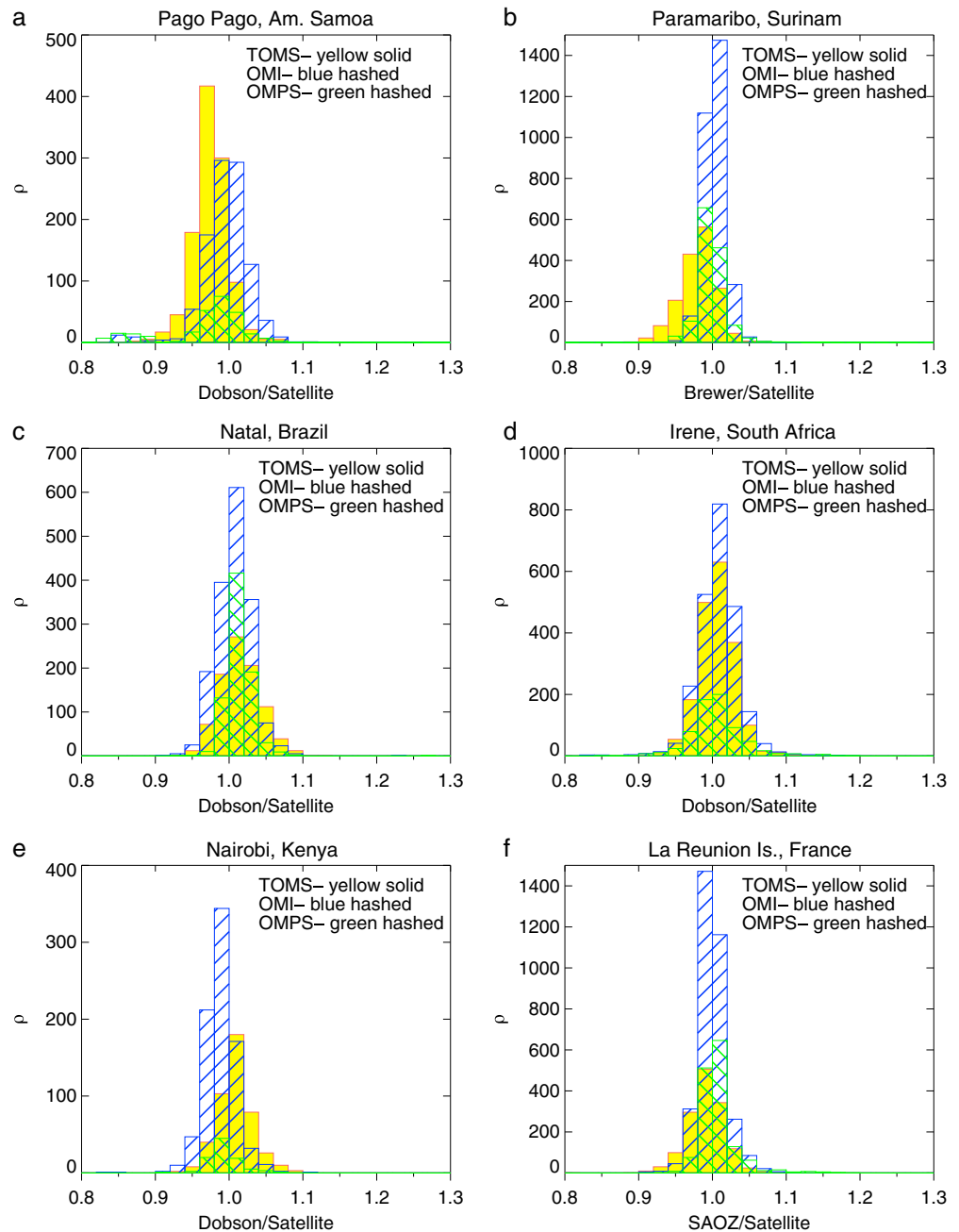
Figure 5. Histograms of the ratio of total column O_3 from the ground-based instruments at nine stations and coincident satellite measurements from TOMS (yellow solid), OMI (blue hashed), OMPS (green hashed). (a) American Samoa; (b) Paramaribo; (c) Natal; (d) Irene; (e) Nairobi; (f) Réunion; (g) Kuala Lumpur; (h) Hanoi; (i) Watukosek.

The Natal record (Figure 4f) displays several data gaps; the hiatus from 2011 to early 2014 was due to equipment malfunction, then obsolescence. As with the Pacific and South American stations (Figures 4a–4e), agreement among sonde, satellites, and Dobson total ozone overall at Natal is very good (Table 3). The histogram of ratios (as percent offset) in Figure 4f (right) averages −1.7% for the composite satellite record (yellow); the Dobson appears to peak slightly lower (hatched in Figure 4f), skewing more negative than the satellite-referenced offsets. Similar to the five stations discussed so far, there is a 2014–2016 dropoff in sonde ratios, consistent among OMI/OMPS and Dobson, at Natal (Figure 4f), even though the instrumentation used at Natal differs from the other stations. The Natal time series during the
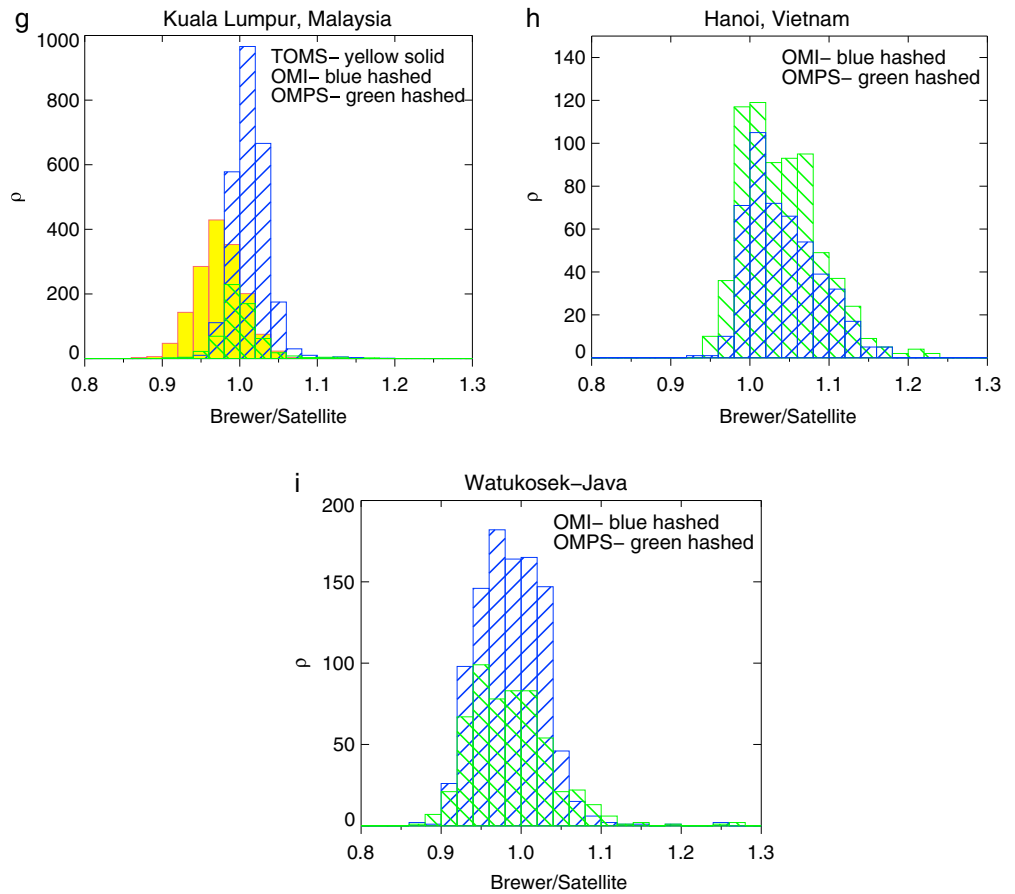
g — Kuala Lumpur, Malaysia (TOMS– yellow solid, OMI– blue hashed, OMPS– green hashed)
h — Hanoi, Vietnam (OMI– blue hashed, OMPS– green hashed)
i — Watukosek–Java (OMI– blue hashed, OMPS– green hashed)

Figure 5. (continued)

Table 3
The Mean and 1 Sigma Standard Deviations of TCO, Stratospheric O_3, and Tropospheric O_3, the Latter Two From the Sondes

Site	Satellite TCO[a]	Ground-based TCO	Sonde TCO (mean satellite Δ, %)	Sonde Stratospheric O_3	Sonde tropospheric O_3	Tropopause (hPa)
Tropical sites within ±19° of equator						
Samoa	251.7 ± 11.0	248.0 ± 10.1	249.4 ± 12.1 (−0.9)	227.9 ± 9.7	21.6 ± 6.3	94.5 ± 13.2
San Cristobal	260.4 ± 12.1	--	258.2 ± 15.0 (−0.9)	231.2 ± 11.9	27.5 ± 10.8	90.6 ± 16.3
Costa Rica	255.7 ± 14.34	--	255.3 ± 19.2 (−0.2)	229.4 ± 17.2	26.0 ± 5.4	94.8 ± 27.4
Paramaribo	262.1 ± 13.8	260.3 ± 12.7	273.0 ± 19.0 (+4.0)	242.1 ± 15.2	30.1 ± 6.8	96.7 ± 22.1
Natal	265.4 ± 11.3	268.8 ± 12.7	260.9 ± 15.1 (−1.7)	226.6 ± 10.1	34.3 ± 8.1	92.9 ± 9.9
Ascension	266.7 ± 10.4	--	260.4 ± 17.9 (−2.4)	221.5 ± 12.5	38.6 ± 8.4	92.8 ± 15.8
Nairobi	260.1 ± 12.4	257.9 ± 13.7	255.8 ± 11.3 (−1.7)	227.2 ± 9.4	28.6 ± 4.9	90.0 ± 14.7
Kuala Lumpur	259.5 ± 13.4	256.6 ± 22.3	246.0 ± 13.5 (−5.5)	220.1 ± 12.8	26.0 ± 5.8	93.3 ± 10.3
Watukosek	257.5 ± 9.5	250.4 ± 10.4	254.3 ± 10.9 (−1.3)	226.9 ± 8.7	27.2 ± 6.8	88.4 ± 8.2
Fiji	258.4 ± 14.5	--	256.0 ± 16.0 (−0.9)	231.0 ± 11.2	24.6 ± 7.9	93.9 ± 11.9
Subtropical sites						
Hilo	273.7 ± 18.4	--	270.4 ± 20.3 (−1.2)	238.8 ± 17.7	31.9 ± 8.0	117.5 ± 41.2
Irene	268.1 ± 15.9	274.6 ± 17.3	273.6 ± 20.0 (+2.0)	237.4 ± 17.3	36.2 ± 6.7	124.5 ± 35.8
La Reunion	267.1 ± 15.1	266.6 ± 14.1	264.8 ± 18.0 (−0.9)	229.6 ± 13.2	35.5 ± 7.8	103.3 ± 25.8
Hanoi	264.7 ± 17.6	276.2 ± 17.6	261.7 ± 21.1 (−1.2)	220.3 ± 18.2	41.2 ± 7.7	91.7 ± 10.8

Note. Values are reported in units of DU. TCO are reported from satellite, ground-based, and ozonesonde instruments. The fourth column includes the percent difference of sonde and satellite mean TCO with respect to sondes. Stratospheric O_3 includes the residual climatology. Sites within ±19° of the equator itemized first from west to east to show the tropospheric wave-one amplitude (sixth column). Subtropical sites follow.
[a]Includes TOMS, OMI, and OMPS TCO overpasses.

TOMS period is unique, with many of the ratios starting out in 1999 and 2000 at 10% lower than the satellite and Dobson (T03; T07). From late 2000 until early 2002, the sonde/TOMS corresponds to 3–4% positive; the sonde also increases relative to the Dobson but mostly remains below 1.0. After early 2002 the sonde-Dobson and TOMS ratios are nearly all below 1.0 again, values that persist to late 2004 to 2006 as the satellite data transition from TOMS to OMI. In mid-2007 and throughout 2008 the sonde ratios relative to both OMI and Dobson become largely >1.0. Natal has >3,300 Dobson-satellite coincidences (Figure 5c) with all three satellite ratios peaking near 1.0.

The instrumentation, preparation technique, and data processing for Ascension (Figure 4g) were the same as at Natal from 1998 to 2010 when the Ascension launches were suspended. Data from 2016 onward are provided by an Ensci/iMet combination instead of Lockheed Martin Sippican (LMS) with SPC (Table 2). The sonde data at Ascension are fairly noisy, and much of the distribution of ratios is skewed to values <0.90 (more negative than 10% in the histogram in Figure 4g). Low ratios are prominent in the beginning of the record, from 1998 to late 2001. After that, from the late TOMS to early OMI period, 2002–2008, there is an increase in the factors, to a majority at >1.0. A short gap follows, after which the values drop to an average ~0.95. After the longer gap, there is a tight clustering between 0.90 and 1.0 (histogram average ~ −5%). The mean sonde-satellite offset is −2.4%.

There was a data gap of more than 4 years in Irene (Figure 4h) largely due to equipment failure. The sonde/satellite and sonde/Dobson ratios are similar; this is also seen in the histograms in Figure 4h (right). Most satellite offsets (yellow in the histogram), range from −2% to +4% with the mean satellite-sonde offset 2.0% (sonde higher, Table 3, fourth column). As with many sonde-satellite comparisons, the ratios in 1998–2001 in the TOMS period are mostly <1.0; this changes to mostly >1.0 in 2002, a value that applies for OMI comparisons in the remainder of the first time series and continues with the OMI and OMPS comparisons with sonde and Dobson from late 2012 to 2016. These variations are consistent with the statistics for satellite and Dobson coincidences at Irene (Figure 5d). However, the Dobson/satellite differences are not large, similar to Natal (Figure 5c), although at Irene, the ratio is slightly smaller for Dobson/TOMS than it is at Natal.

The Nairobi sondes (Figure 4i) are in excellent agreement with the three satellites throughout the 1998–2016 period. The Nairobi histogram (Figure 4i, right) has the highest absolute number of comparisons between sonde and satellites compared to the other sites (scale up to 225). The peak is close to 1.0; the mean offset (Table 3) is −1.7%. During the earliest part of the SHADOZ record, Nairobi (Figure 4i) sonde/satellite and sonde/Dobson ratios are close to unity, which is higher than most of the other stations examined so far. These ratios dip in 2002–2003, then increase in 2004 and even more in the early OMI era. A preponderance of factors >1.0 persists into mid-2010 when there is a short gap. From late 2010 to mid-2014 the sonde ratio relative to OMI and OMPS is close to unity. The Dobson/satellite statistics are summarized in Figure 5e, where the ratios cluster near 1.0; there is less data than for the satellites because of Dobson gaps in 2000–2004 and 2012–2016. The lowest ratios in Figure 5e (blue shading) correspond to the early OMI period (2005–2011) and are consistent with OMI total ozone being greater than TOMS, for which the Dobson ratio peaks slightly higher than 1.0, like Natal and Irene (Figures 5c and 5d).

As described in section 2, the ozone record at La Réunion (Figure 4j) represents further reprocessing since Witte17a. Agreement among the sondes, TOMS, and colocated SAOZ is consistent from 1998 to 2004 with ratios ~0.95 or a mean sonde offset of −5%. During the OMI period from 2005 to 2010, most of the sonde ratios increase to an average ~1.0. In 2011–2012, most factors are >1.0. After 2012 there is a slight dropoff, with a few ratios below 0.9. These variations, taken across the 1998–2016 period, lead to a mean offset of −0.9% for sonde-satellite (yellow in histogram, Figure 4j) and sonde-SAOZ (hatched in histogram). In Figure 5f La Réunion SAOZ/satellite comparisons have a very high sample number, with ratios for all three satellites peaking near 1.0.

For Kuala Lumpur (Figure 4k) from 1998 to 2012, fewer than 10 sonde/satellite ratios were >1.0, but in 2013, there is a jump to many more values >1.0. This is followed by a noisier record with factors both greater and less than 1.0 from late 2013 to early 2016. If it is assumed that the Brewer is a stable reference, the satellite-Brewer total ozone comparisons (Figure 5g) explain these changes. The Brewer/TOMS ratio indicates a higher satellite reading in 1998–2004 than the Brewer, so the sonde/satellite ratios (gray in Figure 4k) are lower than for Brewer. For the OMI period (Brewer is lower than the satellite, Figure 5g), higher sonde/satellite ratios are expected. They increase slightly from 2005 to 2009 (Figure 4k) and much more after the restart of launches in

2012. Most sonde/satellite ratios after 2012 are with OMPS ozone which the Brewer comparison (Figure 5g) suggests measures more ozone than OMI, so many ratios fall to <1.0 (Figure 4k). Sonde offsets from the three satellites average −5.5% (yellow histogram, Figure 4k); the Brewer histogram (hatched in Figure 4k) follows the satellite but with fewer samples.

At Hanoi (Figure 4l, note the late 2004 start) there have been two Brewer instruments (Table 1). The first one spanned the beginning of the sondes in 2004 until 2012, but the noisy data are so divergent from the satellites that we have not used them. Only measurements from the second Brewer, with data from 2012 to 2014, are compared to the sondes; we note that the Brewer/satellite ratios (Figure 5h) are much higher than OMI and OMPS and are outside the guideline for ideal Brewer-satellite agreement (Fioletov et al., 2008). The bottom left panel in Figure 4l, as well as the small sample number in the histogram (hatched, at right), shows that sonde-Brewer coincidences are also infrequent. Sonde-satellite offsets average −1.2%. The Hanoi sonde-satellite data across the OMI and OMPS period until 2014 are fairly consistent (not surprising with similar statistics relative to the Brewer, Figure 5h). From 2014 to 2016 the sonde/satellite ratios are nearly all <1.0. The sonde-satellite histogram in Figure 4l has a long negative tail.

The SHADOZ data at Watukosek (Figure 4m) are compared to a Brewer at Bandung, which is several hundred kilometers to the west and at elevation 740 m (Watukosek is 50 m). Watukosek is also frequently polluted near the surface by local sources (T12; T03). Many Brewer readings have been removed in the comparisons, for example, from 2009 to 2011, because they diverged >10% absolute from the satellite readings. However, those that remain give ratios to OMI and OMPS that are well centered about 1.0 (Figure 5i). The sonde/satellite ratios (Figure 4m, bottom) also average close to 1.0. There is a mean −1.3% offset in the sonde-satellite histogram (yellow in Figure 4m, right, and Table 3).

Fiji has no ground total ozone instrument (Figure 4n), and there are gaps of more than 2 years in the measurement record. For the TOMS and early OMI period, from 1998 to 2005 when the first gap began, sonde/satellite ratios typically fall in the range 0.95–1.0. As for most of the other SHADOZ stations, the sondes record more total ozone than the satellites during the mid-OMI period, 2007–2013. In 2015 the ratios trend lower for both OMI and OMPS, particularly in 2016. The histogram for the satellite comparisons (right, in yellow) skews slightly negative, averaging 0.9% lower for the sondes (Table 3).

3.1.2. Residual Discontinuities in Total Column Ozone Time Series

The discussion of ratios in Figure 4 show that for nearly all of the SHADOZ stations reprocessing has not completely resolved the systematic variability exhibited in the original data (Witte17a). In some cases, quite a bit of noise persists even though the mean TCO is closer to both satellite total ozone and ground-based instruments and is presumed to be more accurate than the original. Section 3.1.1, with satellite-ground-based sonde comparisons over three different satellites, suggests that variations among the satellite sensors (discussed in Witte17b), and perhaps unevenly calibrated Dobsons or Brewers, are two reasons for persistent discontinuities in sonde ratios after reprocessing.

Several additional factors may also contribute. First, there is inherent uncertainty in the ECC sonde measurement, which varies with altitude. This has been evaluated in Witte17b for reprocessed SHADOZ ozone profiles and for the column amounts. Second, the reprocessing prescribed in Smit and ASOPOS (2012) and Deshler et al. (2017) and applied in Witte17a, Witte 17b, and Sterling17 corrects only for variations in the ECC sondes and their operating characteristics. The impact of the many ECC sonde-radiosonde combinations (Table 2) used in SHADOZ has only partially been addressed. For example, additional corrections were made by Witte17a and Sterling17 to compensate for what are assumed to be incorrect pressure readings from iMet radiosondes (Stauffer et al., 2014) at five stations (Table 2). Vertical dashed lines in Figures 4a, 4b, 4d, 4g, and 4n mark the first deployment of the iMet radiosondes at each station. However, these first-order corrections are not based on rigorous lab or field tests with ECC sondes. Looking at distinct changes in the sonde ratios after 2013, their coincidence with the iMet changeover is only straightforward for two data sets. One of those is for Fiji (Figure 4n). The other discontinuity that coincides with iMet is at Ascension (Figure 4g), although the last part of the LMS-SPC instrument combination (2009–2010) also displays sharply lower sonde ratios relative to the record up to 2009. At Samoa, there is a sharp dropoff in ratios at the start of the iMet period (2014 in Figure 4a), but there are clusters with values >1.0 during 2015 and the latter part of 2016. At Hilo (Figure 4b) the falloff in the ratio lags the iMet introduction by about a year; a similar delay is observed for Costa Rica (Figure 4d).
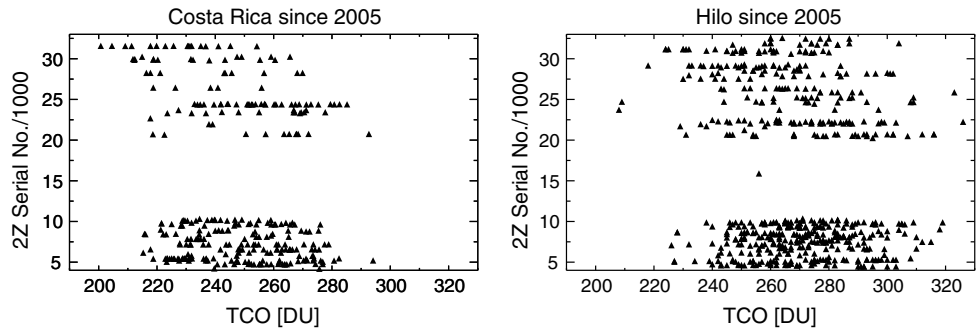
Figure 6. ECC sensor serial number (ENSCI 2Z type divided by 1,000) versus total column O_3 at (left) Costa Rica and (right) Hilo since 2005.

An additional factor in the residual discontinuity of sonde ratios could be the ECC ozonesonde itself. For the six stations using the iMet radiosonde, the coupling is to EnSci/DMT (Droplet Measurement Technology) ECC ozonesondes. This instrument may have been inadvertently modified in the 2011–2016 period as the manufacturer changed, first in 2012 when the original EnSci Corporation became part of Droplet Measurement Technology (DMT), followed by a shift to a new version of the EnSci Corporation in 2016. We tested this hypothesis for four stations that use the Ensci sonde and where the sonde ratio dropped after 2013: Samoa, Hilo, Costa Rica, and Fiji. Several operating characteristics of the sondes, for example, flow rate, background current, and total column ozone, were also examined as a function of the sonde date since 2006, (using the 2Z serial number to track the ECC). Most parameters appeared to be independent of time, except for a lower TCO amount at two stations (Figure 6). Total ozone and the sonde/OMI (OMPS) ratio have dropped off ~15% at Costa Rica since late 2015 (Figure 4d); the relationship to serial number (Figure 6, left) suggests that something might have changed after No. 25000 but there is no clear cause when metadata are examined (this also agrees with findings by H. Vömel, private communication, 2017). At Hilo (Figure 6, right) there have also been a few anomalously low TCO values in 2016, after the 2Z #25000 period. However, analysis of instruments used at Samoa where sonde ratio falloffs after 2014 are observed (Figure 4a), does not show similar behavior. No chamber tests have been carried out over the time of the evolving EnSci instrument. Field tests with the EnSci sondes and the current suite of radiosondes (iMet, RS92, RS41, and LMS) need to be conducted. Moreover, the residual discontinuity in sonde ratios with this first set of reprocessed SHADOZ data is a reminder that the current reprocessing guidelines do not systematically account for radiosonde instrument changes at long-term stations.

3.1.3. Summary of Reprocessed Data and Satellite Total Ozone
Figure 7 summarizes mean total column ozone from TOMS-OMI-OMPS over each SHADOZ station in black (with $\pm 1\sigma$ denoted by the bars). The mean sonde total column ozone value is in red, with the $\pm 1\sigma$ range represented by the pink shading. Table 3 summarizes the corresponding mean sonde-satellite offsets over the 1998–2016 period, except for Costa Rica and Hanoi, where the comparisons are for late 2004 or 2006 to
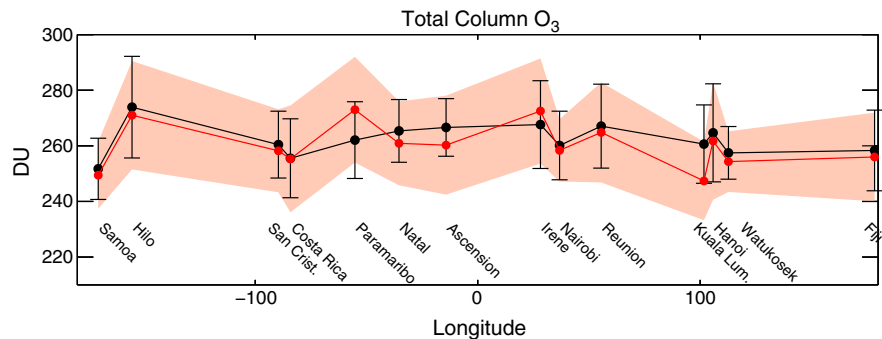
Figure 7. Longitudinal cross section of 1998–2016 reprocessed sonde total column O_3 (red circles with $\pm 1\sigma$ light red shading) and the collective mean TOMS-OMI-OMPS overpass columns (black with $\pm 1\sigma$ black bars). Comparison of total column amounts from the satellites and reprocessed sonde O_3, on average, appear in Table 3, fourth column column.
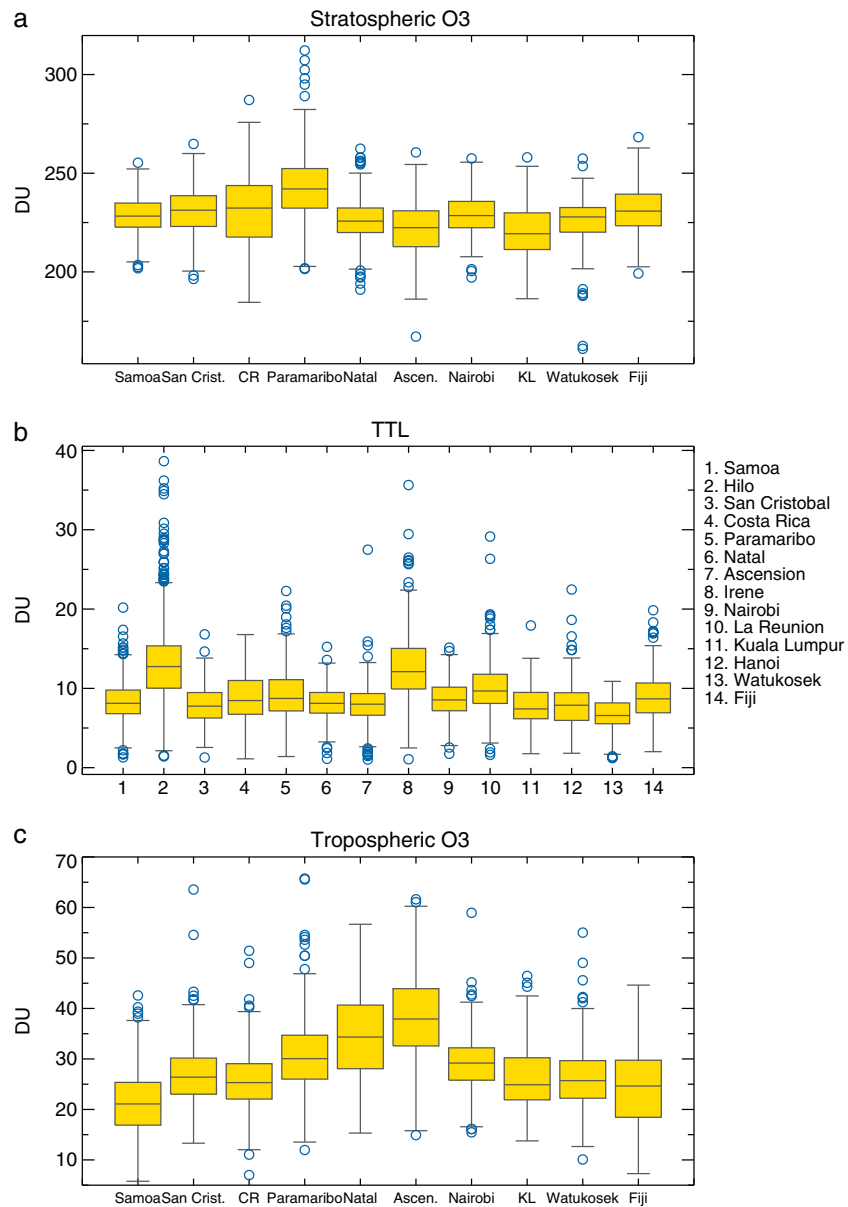
Figure 8. For the 10 tropical SHADOZ stations within ±19° of the equator, box-and-whisker plots of (a) integrated column amounts of stratospheric O_3 (in DU) based on 1998–2016 reprocessed data, (b) TTL column amounts from 15 to 18.5 km (130–70 hPa) for all SHADOZ stations, and (c) tropospheric column amounts integrated from the surface to the tropopause showing the characteristic wave-one pattern. Yellow boxes denote the interquartile ranges.

2016, respectively. For all SHADOZ stations, reprocessing has improved the agreement of the sondes with both the satellites and ground instruments (Figure 11 in T12). With the reprocessed data only two stations display a mean offset > (±)2% (Figures 4 and 7 and Table 3). By contrast, in T07 (Figure 8), sondes for 5 of the 10 stations were offset 5–10% from OMI. Witte17a showed that the greatest improvements in satellite-sonde agreement are for Hanoi and Watukosek (Figure 4l,m); this now applies to reprocessed Réunion, San Cristóbal, and Costa Rica data as well.

3.2. Partial Column Ozone Comparisons, TTL Ozone Structure, and the Tropospheric Wave-One

In prior analyses of SHADOZ column ozone amounts, we computed ozone column amounts within the stratosphere, troposphere, and TTL, along with the structure of the wave-one pattern in tropospheric ozone. Updates to these analyses appear in Figures 8–10. In some of the station-to-station comparisons, as in T12,
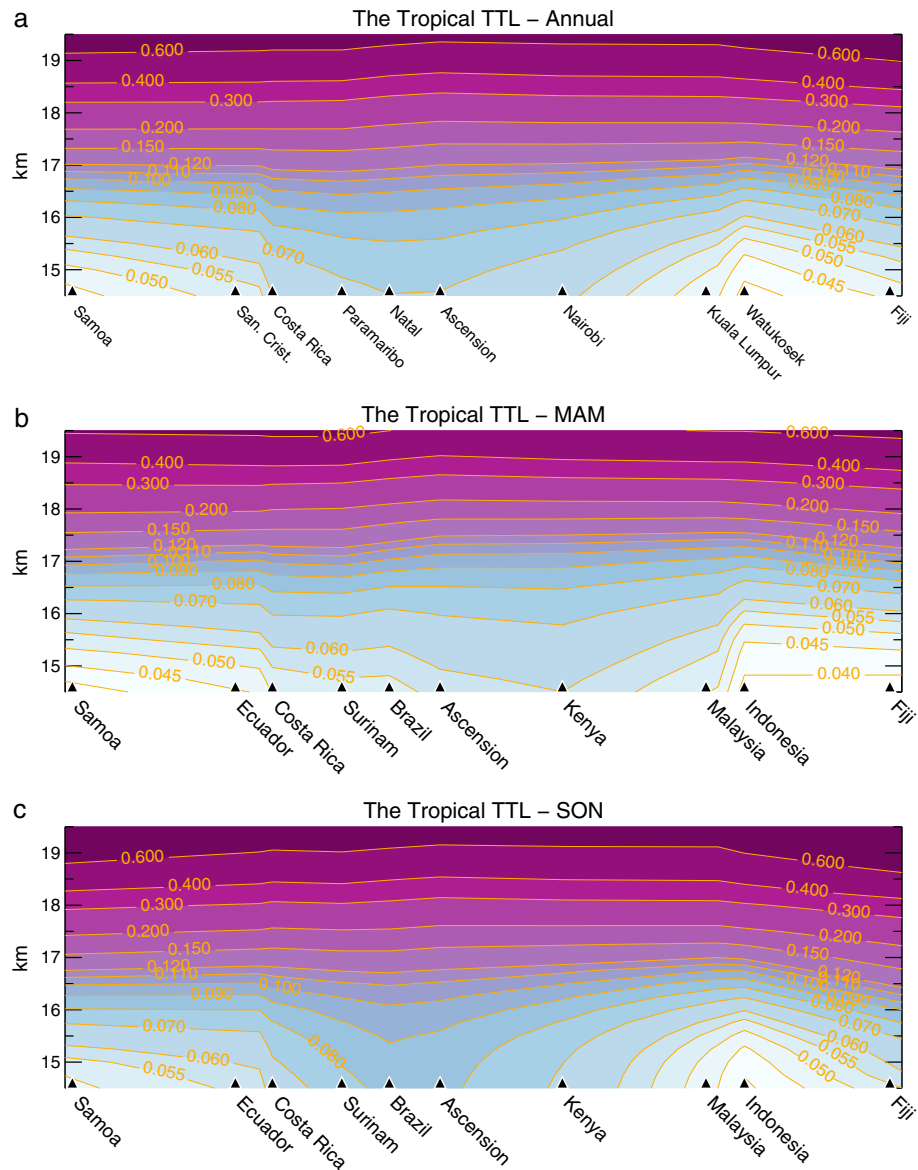
Figure 9. (a) Longitudinal cross section of O_3 mixing ratios (units of ppm), computed from 0.25 km averages of 1998–2016 reprocessed data, for the 10 tropical stations, labeled by station, within the TTL region. (b and c) Same as Figure 9a except for seasons MAM and SON, respectively, and labeled by country. Compared to Figure 8b, where the column amounts are statistically identical, vertical and horizontal gradients in the O_3 structure here are quite pronounced.

we focus on the 10 stations designated as "tropical." The latter sites are distinct from four stations that are subtropical due to seasonally low tropopauses (Baray et al., 1998; Diab et al., 2004; Ogino et al., 2013): Hilo, Irene, Réunion, and Hanoi. The tropopause heights in kilometers for the tropical sites are shown in Figure 3, along with the TTL, here taken as 15–18.5 km or 130–70 hPa.

The stratospheric ozone column, depicted in Figure 8a, obtained by subtracting tropospheric column ozone from total ozone (Table 3), includes the climatological add-on amount above balloon burst. Except for Paramaribo, the other nine tropical stations display a mean of 229 ± 3.9 DU. The relatively small 1σ values shown in Figure 8a represent a significant improvement in data consistency for several stations compared to earlier SHADOZ climatologies (T03; T07; T12). For example, in the first compilation of stratospheric ozone (Table 3, header 7, in T03) the Natal 1σ amount was 9% and in T12 (Table 4) it was 7.5%. This has been reduced to 5% after reprocessing (Figure 8a). There are also absolute percentage changes of this order from T07 (Table 4) compared to the reprocessed data for San Cristóbal, Ascension, Watukosek, and Fiji. In summary,
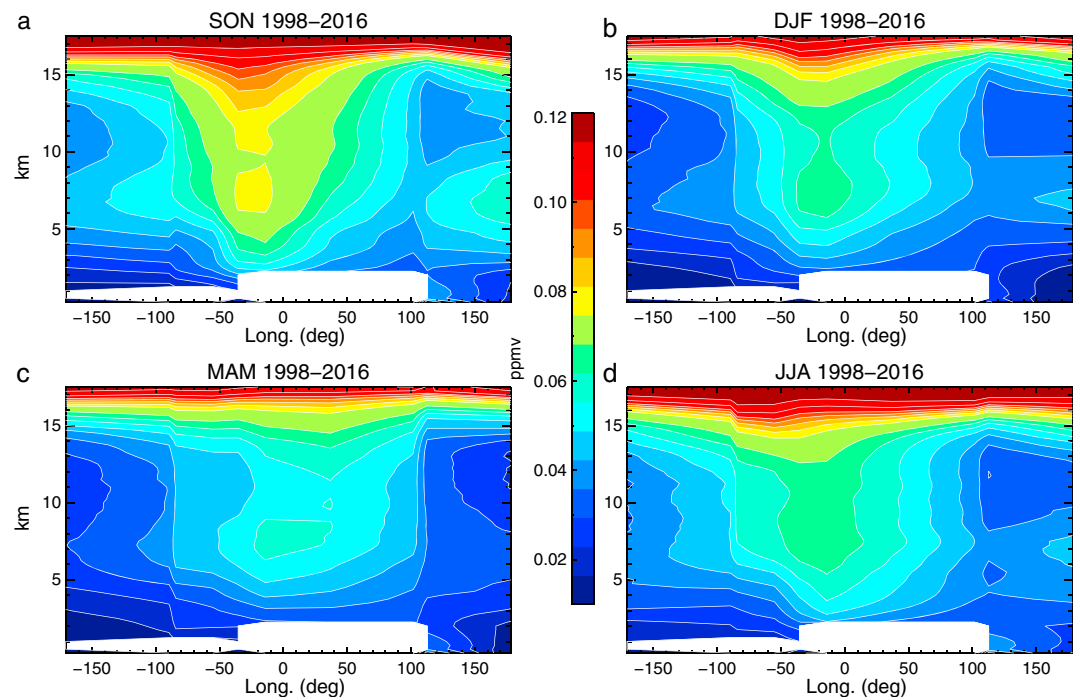
Figure 10. Same as Figure 9, except contours of O$_3$ mixing ratio in the troposphere up to the lower region of the TTL where the wave-one pattern appears, as in T03 and T12. Four seasons illustrated: (a) SON; (b) DJF; (c) MAM; and (d) JJA.

reprocessing has reduced stratospheric column ozone variability (i.e., standard deviation) to 5%. The TCO variability has improved accordingly. Inspection of the ranges and sonde averages (pink edge and red circles in Figure 7) shows that they vary from 4 to 6%.

The TTL column for all 14 SHADOZ stations (Figure 8b) only shows two prominent outliers, Hilo and Irene (numbered 2 and 8, respectively), not surprising because of their subtropical character and expected higher ozone content. They share some of the highest outliers as does the subtropical Réunion station (labeled 10 in Figure 8b). However, Hanoi, also subtropical, does not stand out from the other tropical stations.

A major finding from the SHADOZ data, as described in Thompson, Oltmans, et al. (2011) and Thompson, Witte, Oltmans, et al. (2003) was the isolation of the "wave-one" pattern in total ozone first described by Fishman and Larsen (1987) and Shiotani (1992) (cf. Figure 4 of Kim et al., 1996). For tropical latitudes, the wave-one refers to 10–20 Dobson units (DU) more column ozone over the Atlantic and eastern Africa, a maximum relative to the central western Pacific ozone minimum. The SHADOZ observations from 1998 to 2000 (Thompson, Witte, Oltmans, et al., 2003) demonstrated that because there are no statistically significant differences among column-integrated stratospheric ozone over the individual tropical stations (as in Figure 8a and Table 3), the additional ozone must reside in the troposphere. These findings apply to the reprocessed data from 1998 to 2016 where detailed statistics, in the form of a box-and-whisker plot (Figure 8c) for the 10 tropical stations, are presented. Although Figure 8c does not display station locations realistically, noting from Figure 7 that the wave-one maximum lies between Natal and Ascension, the wave magnitude can be approximated. Based on the data in Figure 8c, the mean tropospheric ozone maximum is ~38 DU. The eastern Indian Ocean-to-Pacific minimum (Figure 8c) extends across four stations from Kuala Lumpur to Samoa, where the range of tropospheric column ozone is 22–26 DU. Taking the mean tropospheric column ozone of 24 DU to represent the zonal minimum, the tropical wave magnitude is estimated as 14 DU. This is the same as estimated in T12.

A cross section of mean TTL mixing ratios, from 15 to 18.5 km, based on 0.25 km averages (Figure 9a), captures nearly uniform ozone mixing ratios above the nominal tropopause (> 17 km) with distinct zonal variations below 16 km. Viewed on a seasonal basis (Figures 9b and 9c), the zonal gradients are more pronounced. In March-April-May (MAM in Figure 9b), a highly convective time of year at most tropical sites, the zonal gradients across 15 km are greater than 50%. The same holds when subsidence and pollution
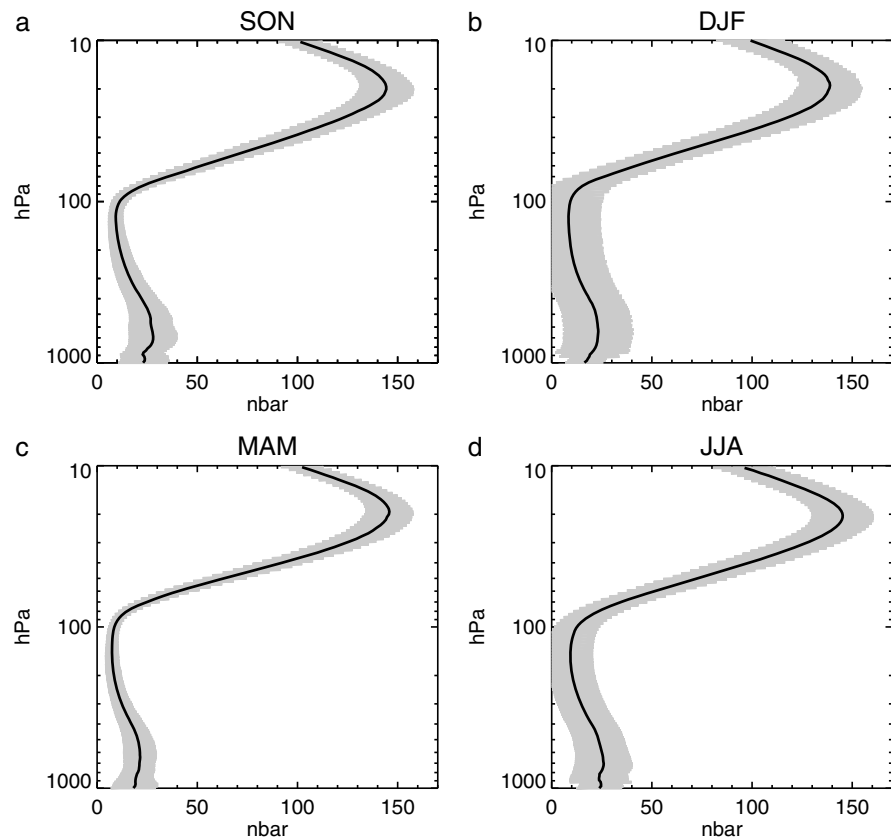
Figure 11. The 1998–2016 seasonally averaged O_3 partial pressure profiles (units of nanobar) for the 10 reprocessed tropical stations. (a) SON; (b) DJF; (c) MAM; and (d) JJA.

impacts in the UT are strongest between Paramaribo and Nairobi (eastern South America to east Africa) in September-October-November (SON in Figure 9c).

Seasonal variations in tropospheric ozone, as in the TTL, cause the wave-one magnitude to vary over the year (Figure 10). As in Thompson, Witte, Oltmans, et al. (2003) Figure 10 indicates that the wave-one is a minimum when most tropical stations are convectively active (MAM). The maximum wave amplitude is observed in SON when there is greater subsidence and pollution sources in the mid-troposphere from Southern Hemisphere biomass fires (T12; Thompson et al., 1996).

3.3. Tropical Station-to-Station Bias

Our prior studies of station-to-station bias focused on the stratosphere because, as Figure 8a implies, the total stratospheric ozone column for the tropical stations is uniform within statistical significance. A mean tropical ozone profile from surface to 10 hPa has been calculated from the 10 most equatorward stations (seasonal means in Figure 11). Note that in Figure 11 the variability of two seasons, DJF (December-January-February) and JJA (June-July-August), is greater than those of MAM and SON (larger 1σ standard deviations, denoted by gray shading) in the troposphere and also near the stratospheric peak. The high variability suggests that it may be difficult to compute reliable trends in the TTL except in SON when ozone is a maximum and in MAM when ozone is a minimum (T03).

When the mean profile for each tropical station is referenced to an all-tropical profile average based on Figure 11, the offsets illustrated in Figure 12 are obtained. Results for the three regions, eastern Indian Ocean to Pacific (labeled as W. Pacific in Figure 12a), eastern Pacific (Figure 12b), and Atlantic plus Nairobi (Figure 12c), are shown separately. It is assumed that above the region marked TTL, stratospheric ozone is zonally invariant and that deviations from 0 signify bias. All the offsets in Figure 12 except for Fiji (blue in Figure 12a) and Ascension near the TTL (red in Figure 12c) are 10% absolute or less. The higher ozone over Fiji below 40 hPa is likely due to subtropical characteristics, perhaps mixing of tropical and midlatitude air,
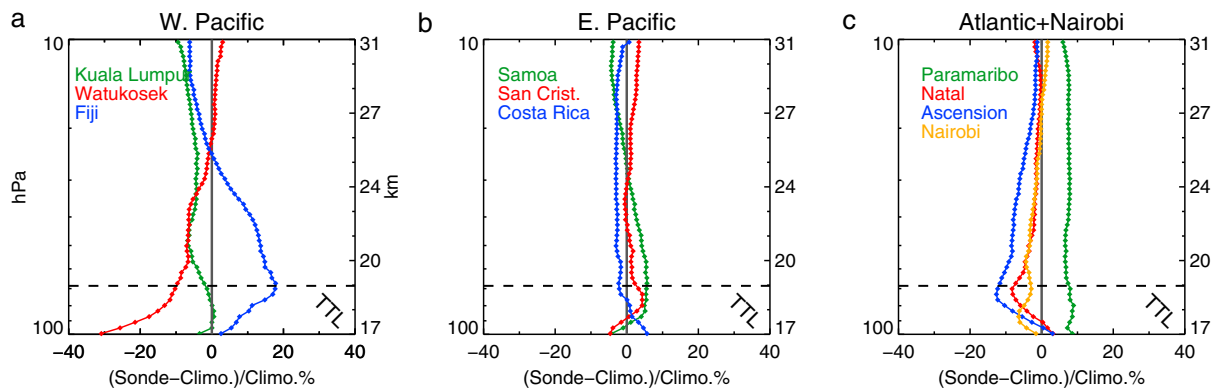
Figure 12. Deviations from the 1998–2016 mean climatological profile from 100 to 10 hPa. TTL upper boundary is marked by the dashed line. Above the TTL, in the stratosphere, station offset differences are more likely to indicate bias. (a) Western Pacific and eastern Indian Ocean stations; (b) Samoa and eastern Pacific; and (c) eastern South America, Ascension, and Nairobi. Station mean profiles are from 1998 to 2016, except for Costa Rica and Hanoi, where launches started in 2004 and 2005, respectively.

in the South Pacific Convergence Zone (the site is at 18°S; Pickering et al., 2001). A nearly identical deviation from the other tropical stations based on 1998–2009 Fiji data appears in Figure 13a of T12. Changes in Watukosek and Kuala Lumpur offsets (Figure 12a) compared to T12 are mostly in the TTL. The three east Pacific stations (Costa Rica grouped with the island sites, Figure 12b) are all close to the mean and show almost no variation throughout the stratosphere. Compared to their T12 offsets, based on 1998–2009 data, Samoa and San Cristóbal in Figure 12b have increased relative to the other stations. Samoa now has a slightly positive offset, and San Cristóbal is close to the zero line. These patterns for Samoa and San Cristóbal are also close to those shown in T07 (Figure 5a) that were based on 1998–2004 observations.

In Figure 12c Nairobi is nearly on the zero line, whereas it had a 5% high bias in T12. This is because reprocessing increases stratospheric ozone at many stations (Witte17a). Paramaribo is consistently high (green in Figure 12c) as in T12. Natal is nearly unchanged from T12, and Ascension is slightly more negative (red and blue, respectively, Figure 12c).

4. Summary

The first set of reprocessed data from 12 SHADOZ stations (1998–2016) and 2 stations (2004–2016) with records covering at least a decade are evaluated in three ways. First, total ozone from the sondes is compared to satellite overpass total ozone from the three BUV-type instrument series that cover the SHADOZ period, EP/TOMS up through 2004, and the operational OMI (since September 2004) and OMPS, since February 2012. Total ozone column coincident with the sondes are also compared to colocated ground-based instruments at nine stations. The main findings are as follows:

1. Reprocessing leads to more consistent total ozone records within a given station except for Paramaribo, which is currently being reprocessed again.
2. Offsets between sonde total ozone and ozone from the satellite series are greatly improved relative to T07 and T12. Two stations register mean absolute sonde-satellite disagreements of 5% absolute; all others are within ±2%. The same applies to sonde TCO agreement with nine colocated ground-based instruments.
3. Although TCO from the sondes, satellites, and ground-based instruments agree better after reprocessing, there is still unexplained noise in most time series of ratios and clear discontinuities when the sonde TCO is compared to the satellite record. The two prominent features are (1) the sonde/satellite TCO record seems to vary among the satellites with TOMS v8 TCO running higher (lowest sonde ratio) than the first 5–7 years of OMI (higher sonde ratio) before the sonde ratio drops during the OMI-OMPS era, and the pattern is confirmed through comparison of the satellite and ground-based instrument TCO; (2) the second discontinuity is observed after 2012–2014 at eight stations with the sonde ratio dropping relative to OMI, OMPS, and, where applicable, the local ground-based instrument. This suggests that something is shifting in the sondes. Radiosonde changes appear to play a role at several stations, and changes in the ECC sonde

can be detected at Costa Rica and Hilo. However, the statistics for the post-2012 drop in sonde ratio are limited compared to a 19 year record for most SHADOZ stations. These patterns are being investigated further. Possible ECC sonde issues will be addressed in JOSIE-type chamber tests in the near future.

The second analysis of the reprocessed data examined three partial column amounts for 10 tropical stations, defined as within 19° latitude absolute: stratospheric ozone, tropospheric ozone, and ozone in the tropical tropopause layer (TTL). As in our prior comparisons (T12; T03; T07) the stratospheric column was zonally invariant except for slightly elevated amounts over Paramaribo. In addition,

1. The TTL column amount is also invariant across the 10 stations (9 ± 1 DU), and two subtropical stations, Réunion and Hanoi, display nearly the same value. However, there is considerable zonal structure below 17 km at all times of year, with strong vertical gradients over the western Pacific and eastern Indian Ocean. These features are not well resolved by profiling satellites, which argues for caution in trends based on satellite data below 70 hPa.
2. The tropospheric wave-one feature first characterized with SHADOZ data from nine stations (Thompson, Witte, Oltmans, et al., 2003) is better delineated with the addition of Costa Rican data. The mean amplitude of the wave is 14 DU.
3. Reprocessing has reduced the standard deviation of stratospheric and total column ozone at SHADOZ stations to 5%.

Third, using mean profiles, we examined midstratospheric bias given that the stratospheric column appears to be zonally invariant among the 10 tropical sites. At all but two stations the bias above 70 hPa has improved relative to the T07 and T12 analyses; the mean for all stations is less than 10% absolute. This demonstrates that key elements in reprocessing procedures, using appropriate pump corrections, applying transfer functions, screening for anomalous background currents, and, in general, applying corrections that account for known biases in the ozonesonde system indeed homogenize SHADOZ data. The results underscore the need for complete metadata in archived sonde records.

Satellite-based tropospheric ozone products and models suitable for exploring complex variability in the tropics are still in development. Given the improvements quantified in this study, we expect reprocessed SHADOZ data to become a standard reference for evaluating new satellites, emerging tropospheric ozone products, and assessment model simulations and for detecting satellite drift. In addition, the seasonal and longitudinal variations in TTL ozone structure observed in SHADOZ data, as well as our classification of tropospheric profiles by self-organizing maps (Jensen et al., 2012; Stauffer et al., 2016), suggest that more attention be given to tropical satellite retrievals below the stratosphere. In the TTL critical interactions take place among ozone, water vapor, temperature, and dynamics; in the free troposphere ozone mediation of OH determines atmospheric lifetimes for myriad species.

Notation

BESOS = Balloon Experiment on Standards for Ozone Sondes
BUV = backscattered ultraviolet
CPT = cold-point tropopause
DJF = December-January-February
DU = Dobson unit; 1 DU = 2.69×10^{16} molecules cm^{-2}
ECC = electrochemical concentration cell
ENSO = El Niño–Southern Oscillation
FT = free troposphere
GOME = Global Ozone Monitoring Experiment (ERS-2 GOME, 1995–2011; GOME II, 2003–, 2012–)
IASI = Infrared Atmospheric Sounder Instrument
IO3C = International Ozone Commission
IGACO = Integrated Global Atmospheric Chemistry Observations
IPCC = Intergovernmental Panel for Climate Change
JJA = June-July-August
JOSIE = Jülich Ozonesonde Intercomparison Experiment (http://www.fz-juelich.de/icg/icg-2/josie)
LS = lower stratosphere

MAM = March–April–May

MLS = Microwave Limb Sounder (on UARS, 1991–2005; on Aura, 2004-)

NASA = National Aeronautics and Space Administration

NDACC = Network for Detection of Atmospheric Composition Change (http://www.ndacc.org)

NOAA = National Oceanic and Atmospheric Administration

NPP = National Polar-Orbiting Partnership

OMI = Ozone Monitoring Instrument (on Aura, 2004-)

OMPS = Ozone Mapper Profiler Suite (on S-NPP, October 2011-)

PTU = Pressure-Temperature-Humidity (data from radiosonde)

QBO = quasi-biennial oscillation

SAOZ = System d'Analyze par Observation Zenitale (http://gosic.org/gcos/SAOZ-prog-overview.html)

SCIAMACHY = Scanning Imaging Absorption SpectroMeter for Atmospheric ChartographY (2002–2012)

SHADOZ = Southern Hemisphere Additional Ozonesondes; (http://tropo.gsfc.nasa.gov/shadoz)

SON = September-October-November

TC^4 = Tropical Composition, Clouds and Climate Coupling; (http://www.espo.nasa.gov/tc4/ (2007))

TOMS = Total Ozone Mapping Spectrometer (in SHADOZ era, Earth-Probe/TOMS, 1996–2005)

TTL = Tropical Tropopause Layer

UT/LS = upper troposphere/lower stratosphere

WMO = World Meteorological Organization

WOUDC = World Ozone and Ultraviolet Data Centre; (http://woudc.org)

References

Baray, J. L., Ancellet, G., Taupin, F. G., Bessafi, M., Baldy, S., & Keckhut, P. (1998). Subtropical tropopause break as a possible stratospheric source of ozone in the tropical troposphere. *Journal of Atmospheric and Solar: Terrestrial Physics*, 60(1), 27–36. https://doi.org/10.1016/S1364-6826(97)00116-8

Bethan, S., Vaughan, G., & Reid, S. J. (1996). A comparison of ozone and thermal tropopause heights and the impact of tropopause definition on quantifying the ozone content of the troposphere. *Quarterly Journal of the Royal Meteorological Society*, 122(532), 929–944. https://doi.org/10.1002/qj.49712253207

Deshler, T., Mercer, J. L., Smit, H. G. J., Stubi, R., Levrat, G., Johnson, B. J., … Sasaki, T. (2008). Atmospheric comparison of electrochemical cell ozonesondes from different manufacturers, and with different cathode solution strengths: The Balloon Experiment on Standards for Ozonesondes. *Journal of Geophysical Research*, 113, D04307. https://doi.org/10.1029/2007JD008975

Deshler, T., Stübi, R., Schmidlin, F. J., Mercer, J. L., Smit, H. G. J., Johnson, B. J., … Nardi, B. (2017). Methods to homogenize electrochemical concentration cell (ECC) ozonesonde measurements across changes in sensing solution concentration or ozonesonde manufacturer. *Atmospheric Measurement Techniques*, 10(6), 2021–2043. https://doi.org/10.5194/amt-10-2021-2017

Diab, R. D., Thompson, A. M., Mari, K., Ramsay, L., & Coetzee, G. J. R. (2004). Tropospheric ozone climatology over Irene, South Africa from 1990–1994 and 1998–2002. *Journal of Geophysical Research*, 109, D20301. https://doi.org/10.1029/2004JD004293

Eyring, V., Harris, N. R. P., Rex, M., Shepherd, T. G., Fahey, D. W., Amanatidis, G. T., … Waugh, D. W. (2005). A strategy for process-oriented validation of coupled chemistry-climate models. *Bulletin of the American Meteorological Society*, 86(8), 1117–1133. https://doi.org/10.1175/BAMS-86-8-1117

Fioletov, V. E., Labow, G., Evans, R., Hare, E. W., Köhler, U., McElroy, C. T., … Weber, M. (2008). Performance of the ground-based total ozone network assessed using satellite data. *Journal of Geophysical Research*, 113, D14313. https://doi.org/10.1029/2008JD009809

Fishman, J., & Larsen, J. C. (1987). Distribution of total ozone and stratospheric ozone in the tropics—Implications for the distribution of tropospheric ozone. *Journal of Geophysical Research*, 92(D6), 6627–6634. https://doi.org/10.1029/JD092iD06p06627

Folkins, I., Braun, C., Thompson, A. M., & Witte, J. C. (2002). Tropical ozone as in indicator of deep convective outflow. *Journal of Geophysical Research*, 107(D13), 4184. https://doi.org/10.1029/2001JD001178

Fortuin, J. P. F., Becker, C. R., Fujiwara, M., Immler, F., Kelder, H. M., Scheele, M. P., … Verver, G. H. L. (2007). Origin and transport of tropical cirrus clouds observed over Paramaribo, Suriname (5.8°N, 55.2°W). *Journal of Geophysical Research*, 112, D09107. https://doi.org/10.1029/2005JD006420

Fueglistaler, S., Dessler, A. E., Dunkerton, T., Folkins, I., Fu, Q., & Mote, P. W. (2009). The tropical tropopause layer. *Reviews of Geophysics*, 47, RG1004. https://doi.org/10.1029/2008RG000267

Fujiwara, M., Hasebe, F., Shiotani, M., Nishi, N., Vömel, H., & Oltmans, S. J. (2001). Water vapor control at the tropopause by equatorial Kelvin waves observed over the Galápagos. *Journal of Geophysical Research*, 28(16), 3143–3146. https://doi.org/10.1029/2001GL013310

Gebhardt, C., Rozanov, A., Hommel, R., Weber, M., Burrows, J. P., Degenstein, D., … Thompson, A. M. (2014). Stratospheric ozone trends and variability as seen by SCIAMACHY from 2002–2011. *Atmospheric Chemistry and Physics*, 14(2), 831–846. https://doi.org/10.5194/acp-14-831/2014

Gettelman, A., & de F. Forster, P. M. (2002). A climatology of the tropical tropopause layer. *Journal of the Meteorological Society of Japan*, 80(4B), 911–924. https://doi.org/10.2151/jmsj.80.911

Heue, K.-P., Coldewey-Egbers, M., Delcloo, A., Lerot, C., Loyola, D., Valks, P., & van Roosendael, M. (2016). Trends of tropical tropospheric ozone from 20 years of European satellite measurements and perspectives for the Sentinel-5 precursor. *Atmospheric Measurement Techniques*, 9(10), 5037–5051. https://doi.org/10.5194/amt-9-5037-2016

Hubert, D., Lambert, J. C., Verhoelst, T., Granville, J., Keppens, A., Baray, J. L., … Zawodny, J. M. (2016). Ground-based assessment of the bias and long-term stability of 14 limb and occultation ozone profile data records. *Atmospheric Measurement Techniques*, *9*(6), 2497–2534. https://doi.org/10.5194/amt-9-2497-2016

Intergovernmental Panel for Climate Change (2007). In S. Solomon, et al. (Eds.), *Climate Change 2007: The Physical Science Basis: Contribution of Working Group I to the Fourth Assessment Report of the Intergovernmental Panel on Climate Change*. Cambridge, UK: Cambridge University Press.

Jensen, A. A., Thompson, A. M., & Schmidlin, F. J. (2012). Classification of Ascension Island and Natal ozonesondes using self-organizing maps. *Journal of Geophysical Research*, *117*, D04302. https://doi.org/10.1029/2011JD016573

Johnson, B. J., Oltmans, S. J., Voemel, H., Smit, H. G. J., Deshler, T., & Kroeger, C. (2002). ECC ozonesonde pump efficiency measurements and tests on the sensitivity to ozone of buffered and unbuffered ECC sensor cathode solutions. *Journal of Geophysical Research*, *107*(D19), 4393. https://doi.org/10.1029/2001JD000557

Kaminski, J., Neary, L., Struzewska, J., McConnell, J. C., Lupu, A., Jarosz, J., … Richter, A. (2008). GEM-AQ, an online global multiscale chemical weather modeling system: Model description and evaluation of gas phase chemistry. *Atmospheric Chemistry and Physics*, *8*(12), 3255–3281. https://doi.org/10.5194/acp-8-3255-2008

Kim, J.-H., Hudson, R. D., & Thompson, A. M. (1996). A new method of deriving time-averaged tropospheric column ozone over the tropics using TOMS radiances: Intercomparison and analysis. *Journal of Geophysical Research*, *101*(D19), 24,317–24,330. https://doi.org/10.1029/96JD01223

Komhyr, W. D. (1969). Electrochemical concentration cells for gas analysis. *Annales Geophysicae*, *25*, 203–210.

Komhyr, W. D. (1986). Operations handbook—Ozone measurements to 40 km altitude with model 4A-ECC-ozone sondes (NOAA Tech. Memorandum, ERL-ARL-149).

Komhyr, W. D., Barnes, R. A., Brothers, G. B., Lathrop, J. A., & Opperman, D. P. (1995). Electrochemical concentration cell ozonesonde performance evaluation during STOIC 1989. *Journal of Geophysical Research*, *100*(D5), 9231–9244. https://doi.org/10.1029/94JD02175

Labow, G. J., Ziemke, J. R., McPeters, R. D., Haffner, D. P., & Bhartia, P. K. (2015). A total ozone-dependent ozone profile climatology based on ozonesondes and Aura MLS data. *Journal of Geophysical Research: Atmospheres*, *120*, 2537–2545. https://doi.org/10.1002/2014JD022634

Liu, G., Liu, J. J., Tarasick, D. W., Fioletov, V. E., Jin, J. J., Moeni, O., … Osman, M. (2013). A global tropospheric ozone climatology from trajectory-mapped ozone soundings. *Atmospheric Chemistry and Physics*, *13*(21), 10,659–10,675. https://doi.org/10.5194/acp-13-10659-2013

Liu, J., Tarasick, D. W., Fioletov, V. E., McLinden, C., Zhao, T., Gong, S., … Moeini, O. (2013). A global ozone climatology from ozone soundings via trajectory mapping: A stratospheric perspective. *Atmospheric Chemistry and Physics*, *13*(22), 11,441–11,464. https://doi.org/10.5194/acp-13-11441-2013

Martin, R. V., Jacob, D. J., Logan, J. A., Bey, I., Yantosca, R. M., Staudt, A. C., Li, Q., & Ginoux, P. (2002). Interpretation of TOMS observations of tropical tropospheric ozone with a global model and in situ observations. *Journal of Geophysical Research*, *107*(D18), 4351. https://doi.org/10.1029/2001JD001480

McPeters, R. D., & Labow, G. J. (2012). Climatology 2011: An MLS and sonde derived ozone climatology for satellite retrieval algorithms. *Journal of Geophysical Research*, *117*(D10), D10303. https://doi.org/10.1029/2011JD017006

McPeters, R. D., Labow, G. J., & Logan, J. A. (2007). Ozone climatological profiles for satellite retrieval algorithms. *Journal of Geophysical Research*, *112*, D05308. https://doi.org/10.1029/2005JD006823

Newton, R., Vaughan, G., Ricketts, H. M. A., Pan, L. L., Weinheimer, A. J., & Chemel, C. (2016). Ozonesonde profiles from the West Pacific Warm Pool: Measurements and validation. *Atmospheric Chemistry and Physics*, *16*(2), 619–634. https://doi.org/10.5194/acp-16-619-2016

Ogino, S.-Y., Fujiwara, M., Shiotani, M., Hasebe, F., Matsumoto, J., Hoang, T. H. T., & Nguyen, T. T. T. (2013). Ozone variations over the northern subtropical region revealed by ozonesonde observations in Hanoi. *Journal of Geophysical Research: Atmospheres*, *118*, 3245–3257. https://doi.org/10.1002/jgrd.50348

Oltmans, S. J., Johnson, B. J., Harris, J. M., Thompson, A. M., Liu, H. Y., Chan, C. Y., … Chang, H.-W. (2004). Tropospheric ozone over the North Pacific from ozonesonde observations. *Journal of Geophysical Research*, *109*, D15S01. https://doi.org/10.1029/2003JD003466

Peters, W., Krol, M. C., Fortuin, J. P. F., Kelder, H. M., Becker, C. R., Thompson, A. M., … Crutzen, P. J. (2004). Tropospheric ozone over a tropical Atlantic station in the Northern Hemisphere: Paramaribo, Surinam (6°N, 55°W). *Tellus B*, *56*(1), 21–34. https://doi.org/10.1111/j.1600-0889.2004.00083.x

Pickering, K. E., Thompson, A. M., Kim, H., DeCaria, A. J., Pfister, L., Kucsera, T. L., … Talbot, R. W. (2001). Trace gas transport and scavenging in PEM-Tropics B South Pacific Convergence Zone convection. *Journal of Geophysical Research*, *106*(D23), 32,591–32,607. https://doi.org/10.1029/2001JD000328

Proffitt, M. H., & McLaughlin, R. J. (1983). Fast response dual-beam UV-absorption photometer suitable for use on stratospheric balloons. *The Review of Scientific Instruments*, *54*, 1719–1728. https://doi.org/10.1063/1.1137316

Randel, W. J., & Thompson, A. M. (2011). Interannual variability and trends in tropical ozone derived from SHADOZ ozonesondes and SAGE II satellite data. *Journal of Geophysical Research*, *116*, D07303. https://doi.org/10.1029/2010JD015195

Sauvage, B., Thouret, V., Thompson, A. M., Witte, J. C., Cammas, J.-P., Nédélec, P., & Athier, G. (2006). Enhanced view of the "tropical Atlantic ozone paradox" and "zonal wave one" from the in situ MOZAIC and SHADOZ data. *Journal of Geophysical Research*, *111*, D01301. https://doi.org/10.1029/2005JD006241

Selkirk, H. B., Vömel, H., Valverde Canossa, J. M., Pfister, L., Diaz, J. A., Fernández, W., … Peng, G. S. (2010). Detailed structure of the tropical upper troposphere and lower stratosphere as revealed by balloon sonde observations of water vapor, ozone, temperature, and winds during the NASA TCSP and TC4 campaigns. *Journal of Geophysical Research*, *115*, D00J19. https://doi.org/10.1029/2009JD013209

Shiotani, M. (1992). Annual, quasi-biennial, and El Niño–Southern Oscillation (ENSO) time-scale variations in equatorial total ozone. *Journal of Geophysical Research*, *97*(D7), 7625–7633. https://doi.org/10.1029/92JD00530

Sivakumar, V., Bencherif, H., Begue, N., & Thompson, A. M. (2011). Tropopause characteristics and variability from 11-year SHADOZ observations in southern tropics and subtropics. *Journal of Applied Meteorology and Climatology*, *50*(7), 1403–1416. https://doi.org/10.1175/2011JAMC2453.1

Smit, H. G. J, & Kley, D. (1998). JOSIE: The 1996 WMO international intercomparison of ozonesondes under quasi flight conditions in the environmental simulation chamber at Jülich, WMO/IGAC-Report, WMO Global Atmosphere Watch report series, No. 130 (Technical Document No. 926). Geneva: World Meteorological Organization.

Smit, H. G. J., & Panel for the Assessment of Standard Operating Procedures for Ozonesondes (ASOPOS) (2012). Guidelines for homogenization of ozonesonde data, SI2N/O3S-DQA activity as part of "past changes in the vertical distribution of ozone assessment". Retrieved from http://www-das.uwyo.edu/%7Edeshler/NDACC_O3Sondes/O3s_DQA/O3S-DQA-Guidelines%20Homogenization-V2-19November2012.pdf

Smit, H. G. J., & Panel for the Assessment of Standard Operating Procedures for Ozonesondes (ASOPOS) (2014). Quality assurance and quality control for ozonesonde measurements in GAW, World Meteorological Organization (GAW Report #201). Retrieved from http://www.wmo.int/pages/prog/arep/gaw/documents/FINAL_GAW_201_Oct_2014.pdf

Smit, H. G. J., & Straeter, W. (2004). JOSIE-1998, performance of ECC ozone sondes of SPC-6A and ENSCI-Z type, WMO Global Atmosphere Watch report series, No. 157 (Technical Document No. 1218). Geneva: World Meteorological Organization.

Smit, H. G. J., Straeter, W., Johnson, B. J., Oltmans, S. J., Davies, J., Tarasick, D. W., … Posny, F. (2007). Assessment of the performance of ECC-ozonesondes under quasi-flight conditions in the environmental simulation chamber: Insights from the Juelich Ozone Sonde Intercomparison Experiment (JOSIE). *Journal of Geophysical Research*, *112*, D19306. https://doi.org/10.1029/2006JD007308

Stauffer, R. M., Morris, G. A., Thompson, A. M., Joseph, E., Coetzee, G. J. R., & Nalli, N. R. (2014). Propagation of radiosonde pressure sensor errors to ozonesonde measurements. *Atmospheric Measurement Techniques*, *7*(1), 65–79. https://doi.org/10.5194/amt-7-65-2014

Stauffer, R. M., Thompson, A. M., & Young, G. S. (2016). Tropospheric ozonesonde profiles at long-term U.S. monitoring sites: 1. A climatology based on self-organizing maps. *Journal of Geophysical Research: Atmospheres*, *121*, 1320–1339. https://doi.org/10.1002/2015JD023641

Stevenson, D. S., Dentener, F. J., Schultz, M. G., Ellingsen, K., van Noije, T. P. C., Wild, O., … Szopa, S. (2006). Multimodel ensemble simulations of present-day and near-future tropospheric ozone. *Journal of Geophysical Research*, *111*, D08301. https://doi.org/10.1029/2006JD006338

Takashima, H., & Shiotani, M. (2007). Ozone variation in the tropical tropopause layer as seen from ozonesonde data. *Journal of Geophysical Research*, *112*, D11123. https://doi.org/10.1029/2006JD008322

Tarasick, D. W., Davies, J., Smit, H. G. J., & Oltmans, S. J. (2016). A re-evaluated Canadian ozonesonde record: Measurements of the vertical distribution of ozone over Canada from 1966 to 2013. *Atmospheric Measurement Techniques*, *9*(1), 195–214. https://doi.org/10.5194/amt-9-195-2016

Tarasick, D. W., Jin, J. J., Fioletov, V. E., Liu, G., Thompson, A. M., Oltmans, S. J., … Thouret, V. (2010). High-resolution tropospheric ozone fields for INTEX and ARCTAS from IONS ozonesondes. *Journal of Geophysical Research*, *115*, D20301. https://doi.org/10.1029/2009JD012918

Thompson, A. M., Allen, A. L., Lee, S., Miller, S. K., & Witte, J. C. (2011). Gravity and Rossby wave signatures in the tropical troposphere and lower stratosphere based on Southern Hemisphere Additional Ozonesondes (SHADOZ), 1998–2007. *Journal of Geophysical Research*, *116*, D05302. https://doi.org/10.1029/2009JD013429

Thompson, A. M., Balashov, N. V., Witte, J. C., Coetzee, G. J. R., Thouret, V., & Posny, F. (2014). Tropospheric ozone increases in the southern African region: Bellwether for rapid growth in Southern Hemisphere pollution? *Atmospheric Chemistry and Physics*, *14*(18), 9855–9869. https://doi.org/10.5194/acp-14-9855-2014

Thompson, A. M., Doddridge, B. G., Witte, J. C., Hudson, R. D., Luke, W. T., Johnson, J. E., … Weller, R. (2000). A tropical Atlantic paradox: Shipboard and satellite views of a tropospheric ozone maximum and wave-one in January–February 1999. *Geophysical Research Letters*, *27*(20), 3317–3320. https://doi.org/10.1029/1999GL011273

Thompson, A. M., MacFarlane, A. M., Morris, G. A., Yorks, J. E., Miller, S. K., Taubman, B. F., … Hlavka, D. L. (2010). Convective and wave signatures in ozone profiles over the equatorial Americas: Views from TC4 2007 and SHADOZ. *Journal of Geophysical Research*, *115*, D00J23. https://doi.org/10.1029/2009JD012909

Thompson, A. M., Miller, S. K., Tilmes, S., Kollonige, D. W., Witte, J. C., Oltmans, S. J., … Ha, H. T. T. (2012). Southern Hemisphere Additional Ozonesondes (SHADOZ) tropical ozone climatology: Tropospheric and tropical tropopause layer (TTL) profiles with comparisons to OMI-based ozone products. *Journal of Geophysical Research*, *117*, D23301. https://doi.org/10.1029/2010JD016911

Thompson, A. M., Oltmans, S. J., Tarasick, D. W., Von der Gathen, P., Smit, H. G. J., & Witte, J. C. (2011). Strategic ozone sounding networks: Review of design and accomplishments. *Atmospheric Environment*, *45*(13), 2145–2163. https://doi.org/10.1016/j.atmosenv.2010.05.002

Thompson, A. M., Pickering, K. E., McNamara, D. P., Schoeberl, M. R., Hudson, R. D., Kim, J. H., … Nganga, D. (1996). Where did tropospheric ozone over southern Africa and the tropical Atlantic come from in October 1992? Insights from TOMS, GTE TRACE A, and SAFARI 1992. *Journal of Geophysical Research*, *101*(D19), 24,251–24,278. https://doi.org/10.1029/96JD01463

Thompson, A. M., Witte, J. C., McPeters, R. D., Oltmans, S. J., Schmidlin, F. J., Logan, J. A., … Labow, G. (2003). Southern Hemisphere Additional Ozonesondes (SHADOZ) 1998–2000 tropical ozone climatology 1. Comparison with Total Ozone Mapping Spectrometer (TOMS) and ground-based measurements. *Journal of Geophysical Research*, *108*(D2), 8238. https://doi.org/10.1029/2001JD000967

Thompson, A. M., Witte, J. C., Oltmans, S. J., Schmidlin, F. J., Logan, J. A., Fujiwara, M., … Kelder, H. M. (2003), Southern Hemisphere Additional Ozonesondes (SHADOZ) 1998–2000 tropical ozone climatology 2. Tropospheric variability and the zonal wave-one. *Journal of Geophysical Research*, *108*(D2), 8241. https://doi.org/10.1029/2002JD002241

Thompson, A. M., Witte, J. C., Smit, H. G. J., Oltmans, S. J., Johnson, B. J., Kirchhoff, V. W. J. H., & Schmidlin, F. J. (2007). Southern Hemisphere Additional Ozonesondes (SHADOZ) 1998–2004 tropical ozone climatology: 3. Instrumentation, station-to-station variability, and evaluation with simulated flight profiles. *Journal of Geophysical Research*, *112*, D03304. https://doi.org/10.1029/2005JD007042

Thouret, V., Saunois, M., Minga, A., Mariscal, A., Sauvage, B., Solete, A., … Schlager, H. (2009). An overview of two years of ozone soundings over Cotonou as part of AMMA. *Atmospheric Chemistry and Physics*, *9*(16), 6157–6174. https://doi.org/10.5194/acp-9-6157-2009

Tilmes, S., Lamarque, J.-F., Emmons, L. K., Conley, A., Schultz, M. G., Saunois, M., … Tarasick, D. (2012). Technical note: Ozonesonde climatology between 1995 and 2011: Description, evaluation and applications. *Atmospheric Chemistry and Physics*, *12*(16), 7475–7497. https://doi.org/10.5194/acp-12-7475-2012

van Malderen, R., Allaart, M. A. F., De Backer, H., Smit, H. G. J., & De Muer, D. (2016). On instrumental errors and related correction strategies of ozonesondes: Possible effect on calculated ozone trends for the nearby sites Uccle and De Bilt. *Atmospheric Measurement Techniques*, *9*(8), 3793–3816. https://doi.org/10.5194/amt-9-3793-2016

Vömel, H., Oltmans, S. J., Johnson, B. J., Hasebe, F., Shiotani, M., Fujiwara, M., & Enriquez, H. (2002). Balloon-borne observations of water vapor and ozone in the tropical upper troposphere and lower stratosphere. *Journal of Geophysical Research*, *107*(D14), 4210. https://doi.org/10.1029/2001JD000707

Witte, J. C., Thompson, A. M., Smit, H. G. J., Fujiwara, M., Posny, F., Coetzee, G. J. R., … da Silva, F. R. (2017). First reprocessing of Southern Hemisphere ADditional Ozonesondes (SHADOZ) profile records (1998–2015): 1. Methodology and evaluation. *Journal of Geophysical Research: Atmospheres*, *122*, 6611–6636. https://doi.org/10.1002/2016JD026403

World Meteorological Organization (WMO) (2007). Scientific assessment of ozone depletion: 2006 (Global Ozone Research and Monitoring Project - Report No. 50, 572 pp.). Geneva.

World Meteorological Organization (WMO) (2011). Scientific assessment of ozone depletion: 2010 (Global Ozone Research and Monitoring Project - Report No. 52, 516 pp.). Geneva.

World Meteorological Organization (WMO) (2014). Scientific assessment of ozone depletion: 2014 (Global Ozone Research and Monitoring Project - Report No. 55, 416 pp.). Geneva.

Yonemura, S., Tsuruta, H., Kawashima, S., Sudo, S., Peng, L. C., Fook, L. S., … Hayashi, M. (2002). Tropospheric ozone climatology over peninsular Malaysia from 1992 to 1999. *Journal of Geophysical Research*, *107*(D15), 4229. https://doi.org/10.1029/2001JD000993